M.A. LATYPOVA* and Z.S. GELMANOVA
Karaganda Industrial University,
30 Republic Ave., 101400 Temirtau, Kazakhstan

* m.latypova@tttu.edu.kz

ORDERING ALLOYS WITH MICRO- AND NANOSCALE STRUCTURES BASED ON CUBIC LATTICES: MECHANICAL AND THERMODYNAMIC PROPERTIES

The development of the transport, chemical, and energy industries, aerospace engineering, and shipbuilding dictates the need to develop and create new materials capable of functioning in various conditions. These materials include atomically ordered alloys based on the noble metals with specific properties such as high corrosion resistance, low electrical resistance, and suitable magnetic and optical properties. At the same time, for their practical application, an integrated combination of the necessary operational characteristics is becoming increasingly in demand, providing sufficient electrical resistive and electrical contact properties, high strength and plasticity in addition to the corrosion resistance. Simultaneously, the simplicity of the chemical composition of the materials being created or improved, the manufacturability of the metallurgical process, and subsequent production conversions on existing equipment remain undoubtedly important.

Keywords: long-range atomic order, ordered alloys, kinetics, deformation mechanism, microstructure.

1. Introduction

In the 20th century, due to the rapidly increasing needs of the developing industry in various structural and functional metal materials, new technologies were continuously created, and new alloy steels and alloys were developed. The number of principal alloying elements and their share in

the total mass of materials gradually increased. Some grades of applied steels and alloys, primarily stainless, heat-resistant, high-strength, already contained 4−5 controlled principal alloying elements weighing up to 30−40%, high-strength aluminium alloys with 3−4 elements by weight up to 10−15%, brass and bronze — up to 40 and 15%, respectively. In the intermetallics, which make up an extensive class of atomically ordered compounds of the initial metal elements, on the contrary, 2−3 main material-forming metals were used, but in high concentrations: 25−75% in compounds of type A_3B, up to 50% in compounds of type AB or A_2BC. Ordered by various types ($A15$, $B2$, $C15$, $D0_3$, $L1_0$, $L1_2$, $L2_1$, *etc.*), often without good structural and technological characteristics, intermetallides had particular functional properties: superconductivity (Nb_3Sn, V_3Ga), magnetism (Fe, Ni, Co compounds), heat resistance (NiAl, CoAl, CoNiAl), heat resistance (Ni_3Al, Ti_3Al, TiAl), shape memory effects, thermally, deformationally or magnetically controlled (TiNi, Ni_2MnGa, *etc.*).

A significant improvement in the complex structural, functional, and technological parameters of alloys and intermetallics was associated with additional micro- and macro-alloying (third, fourth, fifth, and sixth elements), the development of special hardening and plasticizing technologies for both synthesis and subsequent processing of poly- and single crystals, modification of their micro- and sub microcrystalline structures. At the beginning of the 21st century, work began on the creation and comprehensive research of new so-called high-entropy polymetallic alloys, including 5−6 or more basic elements [1−25].

One of the transformations underlying the latest technologies for creating functional and structural materials is the atomic ordering of alloys. Changes in the degree of perfection of the crystal lattice, associated with the processes of arrangement (cluster formation) of atoms in metals, significantly affect their properties: structural, mechanical, thermal, electrical, magnetic, and optical. Therefore, during the ordering process, it is possible to obtain a set of properties that optimally combines, *e.g.*, low electrical resistance, high strength, and the necessary magnetic and optical characteristics [26]. The use of ordered alloys as functional or structural materials is attractive because changing the degree of order (parameter of atomic order) makes it possible to regulate that set of material qualities. Different types of alloys' processing are used to create the necessary states of atomic order, which can be both equilibrium and metastable or non-equilibrium at all (obtained, in particular, as a result of quenching) [27].

In addition to purely metallurgical problems, the study of atomic ordering raises questions that are important for understanding the fundamental aspects of solid-state physics. For many decades, studies of (mainly binary) alloys have been carried out. In numerous works, the types of ordered crystal structures, points of phase transformations, regions of

phase stability, transitions from distant order to purely close order and vice versa, the influence of (non)equilibrium states realized during order–disorder phase transformations on the properties of materials were studied [26]. Some issues of atomic ordering kinetics as well as effects of ordering on the evolution of material properties have been studied. Many monographies and reviews [26–55] (see also references in Refs. [26, 51]) deal with the atomic ordering of alloys and summarize theoretical and experimental studies of the nature of this phenomenon, the bibliography of which reaches several thousand publications.

Alloys based on gold and platinum group metals, despite the high cost, play an increasingly prominent role in our daily lives. That applies not only to jewellery, where, along with gold alloys, the demand for platinum and palladium products is growing. The pins of the microcircuits are coated with gold, and glass is sprayed to give it athermal properties. Alloys based on gold, platinum, and palladium are used in medicine, for example, dentistry and acupuncture. Every year, the consumption of platinum and palladium in the automotive industry increases for the manufacture of catalytic converters, which protect the atmosphere from toxic exhaust gases. And, of course, the use of precious metal alloys in engineering, in critical assemblies and devices remains, where they have found application as contact, resistive, spring, and magnetically rigid materials.

The field of application of precious metal-based alloys is constantly expanding: recently, prospects for using Fe–Pd, Fe–Pt, and Co–Pt systems in computer technologies as a nanocrystalline medium for high-density magnetic recording of information have been revealed. In addition, it turned out that FePd and FePt alloys have a 'magnetic shape memory', *i.e.*, they allow for large reversible deformations due to the restructuring of the magnetic domain structure in a magnetic field.

The ever-growing interest in gold and palladium-based alloys urgently requires a broad fundamental study of the formation of their structure and properties to solve emerging technological problems. For practical use, first of all, it is necessary to create a set of optimal properties in alloys. Moreover, for successful application in a particular field, the set of such properties may be different. However, a general requirement is the presence of high strength in alloys with sufficient plasticity.

Most precious metal-based alloys are ordered, *i.e.*, when cooled below a certain critical temperature (T_c), the different atoms that make up the alloy occupy strictly defined places in the crystal lattice. Such ordered states are commonly called superstructures. Ordered alloys are very close to intermetallics, in which the atomic long-range order is formed directly from the melt. Intermetallides have several unique properties, primarily an abnormal temperature dependence of the yield point, *i.e.*, they demonstrate an increase in the yield strength when heated in a certain temperature range. That is why some intermetallics have become the basis of

several aerospace materials, while others are considered promising for developing new functional materials.

Thus, the research continuation on the formation of microstructure and the kinetics of ordering, the features of the deformation behaviour of gold and palladium-based alloys pursues a dual goal. On the one hand, this will give an impetus to solving several technological issues, which will further improve (optimize) the properties of alloys already used in the industry. On the other hand, it will help to understand the nature of temperature anomalies observed in intermetallics and may lead to the creation of new materials.

Of particular interest are the $L1_0$-, $L1_2$-, and $B2$-type superstructures, which are formed by the vast majority of ordered alloys. The $L1_0$-type superstructure has a tetragonal lattice and two other superstructures. The $L1_0$ superstructure is formed in a large group of binary alloys (CuAu, CoPt, NiPt, FePd). In the disordered state, they have an f.c.c. lattice, in the ordered state they have an f.c.t. one, in which the planes (001) are alternately filled with atoms of the same type. The degree of tetragonality of a given superlattice is usually determined by the ratio of the axes of translations of the unit cell c/a. Due to the shape change of the cell during ordering, large elastic stresses arise in the alloy, which stimulates the formation of a lamellar structure consisting of colonies of lamellar c-domains articulating with each other along planes of type $\{110\}$.

All the alloys listed above have already been studied in detail. Moreover, it was in the gold–copper system that the ordered state of atoms in the crystal lattice was discovered. A large number of papers have been devoted to the peculiarities of the formation of microstructure during the order–disorder transitions in the CuAu equiatomic alloy [56]. Nevertheless, several issues were either not raised at all or were discussed only theoretically, without setting up appropriate experiments. For example, in most studies, the ordering processes were studied in recrystallized material obtained either by slow cooling from a temperature above critical or by annealing after quenching from a high-temperature region.

The formation of the microstructure of alloys during ordering after preliminary plastic deformation has remained practically not considered. As explained in Ref. [57], in this case, 'the recrystallization of the alloy is carried out below the phase transition temperature and strongly depends on the initial degree of deformation, heating rate, temperature, holding time and subsequent cooling mode and it seems difficult to take into account so many variable conditions during the experiment'.

The results presented in Refs. [58, 59] reflect the complex nature of this phenomenon and the difficulties in its interpretation. Indeed, when annealing below T_c after preliminary plastic deformation, two diffusion processes must occur in the material: recrystallization and ordering. Existing theoretical works predict some interesting features of the forma-

tion of the alloy microstructure during ordering after preliminary plastic deformation. Depending on the temperature range, in which annealing is performed, these processes can occur either together, or one of them may be ahead of the other. Of particular interest is the situation when ordering outstrips recrystallization. In this case, most of the dislocations inherited from the initially deformed state lose their mobility and become, as it were, 'frozen' into an ordered structure, forming a kind of framework.

Previously, it was experimentally discovered that for almost all alloys with the $L1_0$ superstructure, there is a temperature range and annealing inside which, after preliminary plastic deformation, leads to the forming of a particular structural state. In this state, NiPt, CoPt and FePd alloys successfully combine high strength and plastic properties, so it was called optimal [60, 61]. These works mainly concerned the study of the mechanical properties of alloys, without analysing the interrelationship of various phenomena and developing a common approach. Before this work, there was no model explaining the occurrence of an optimal structural state in L10 superstructures. In addition, it was unknown whether it was possible to achieve a similar state in other superstructures.

The experimenters also ignored, that a temperature anomaly of the yield point has not yet been detected for alloys with the $L1_0$ superstructure. At the same time, the intermetallic TiAl compound, which has the same superstructure, demonstrates an abnormal dependence on temperature, which is used in engineering. The question arises: is the presence of this anomaly in TiAl a property of a specific material (intermetallide) or perhaps this effect cannot be detected on alloys with the $L1_0$ superstructure for some reason?

Separately, we should focus on the problem of obtaining a monodomain alloy crystal with $L1_0$-type superstructure. The formation of a single c domain in the entire monocrystalline sample with an $L1_0$ superstructure is of particular interest, since in such alloys, because of ordering, a lamellar structure is usually formed with a large number of c domain boundaries of various orientations. When studying such a structure, it is hard to separate the effects arising from the influence of boundaries from the properties of the volume of the domain itself. Thus, the task arises of designing an experimental setup and studying the structure of the monocrystalline samples obtained on it.

The $B2$-type superstructure is formed in alloys of the Cu (35−50 at.%) type system. These alloys are interesting because, during the disorder−order phase transition, the crystal lattice in them changes from f.c.c.-disordered state to b.c.c.-ordered one. Since domain boundaries are not formed in this case, the most effective way to harden alloys of this system is considered grain grinding during phase recrystallization with forward and reverse order−disorder transformation. The possibility of increasing the strength properties through ordering after preliminary plastic deformation on this system was practically not considered.

To solve this issue, first of all, information on the kinetics of phase transitions in this system is needed. However, it turned out that only fragmentary information on this issue is available in the literature. Thus, the order rate in this system was studied on alloys with a palladium content from 44 to 50 at.%, *i.e.*, close to equiatomic. At the same time, the Cu–40 at.% Pd alloy is of the greatest interest from the point of view of obtaining a complex of high strength and plastic properties. In the published works, there are completely different estimates of the ordering rate of this alloy, which differ hundreds of times and require verification. In addition, it is indicated in that several maxima are observed on the curve of isothermal transformations of the Cu–40 Pd alloy describing the process of disordering, which has not yet been confirmed by other researchers. Thus, it is interesting to study further the features of the microstructure formation and mechanical properties in the process of $A1$–$B2$ phase transformations in the Cu–Pd alloy [62].

It is known that in the near-order state, some palladium-based alloys exhibit an abnormal dependence of electrical resistance on temperature: PdW, PdMo, PdAg. Due to this phenomenon, Pd–Ag alloy is used in engineering as a contact or strain gauge material, the state of the short-range order was repeatedly recorded earlier in the copper-palladium system, but no anomalies were detected. Since this alloy has a very low electrical resistivity in an ordered state, it is interesting to find out whether there is a temperature anomaly p in this alloy. This would make it possible to obtain a material with high electrical conductivity over a wide temperature range.

The main modern methods for improving the mechanical properties of metal alloys include methods that provide nanostructural hardening due to the formation of a dislocation substructure, the decomposition of a supersaturated solid solution with the formation of highly dispersed precipitates, a domain substructure in atomically ordered alloys and, finally, the grinding of the grain structure of polycrystals down to the nanoscale scale. Sometimes, it is effective to combine different hardening mechanisms in one metal alloy. Thus, in several alloys, intense megaplastic deformation (MPD) can provide the formation of ultrafine-grained structural states with a grain size of nanocrystallites from 10 to 100 nm. However, if the effect of MPD has been studied in great detail over the past 20–30 years on a wide variety of metal systems (pure metals, model, and industrial alloys) [33–45], then, such systematic studies on atomically ordered alloys, especially for special industrial purposes, are practically absent.

As known [63–78], the most common methods for obtaining materials for structural and functional purposes are based on the widespread use of structural and phase transformations in alloys. There are three groups of the substitutional metallic solid solutions. The first includes disordered solid solutions, in which the atoms of the components statistically randomly or chaotically occupy the sites of the crystal lattice. The second

consists of solutions with short-range atomic order, in which the atoms of the first component prefer the atoms of the second component as neighbouring atoms. The third includes cluster solutions, in which, on the contrary, the first component prefers atoms of the same type as neighbours.

2. Features of Ordered Alloys

In intermetallic compounds, the first and other components occupy orderly strictly defined sites of the crystal lattice or sublattice. Alloys with an order−disorder phase transition behave like intermetallic compounds at low temperatures but turn into disordered solid solutions with a possible near atomic order above a certain temperature below the melting point. This temperature is called the critical temperature T_c. For example, alloys with a structure close to the stoichiometric composition corresponding to the formula A_3B are described in an unordered state by the f.c.c. lattice, at all sites of which atoms of type A or B. Therefore, in an ordered state, the sites legitimate for atom A are the vertices of cubic cells, and for atom B are the centres of the faces of these cells.

The most fully investigated alloys of this type include alloys of the Au−Cu system near the composition $AuCu_3$ [77]. These alloys with a stoichiometric composition are ordered when a quasi-equilibrium state is reached below the temperature of $T_c \approx 665$ K. When moving away from the stoichiometric composition in both directions, the ordering temperature, as experience shows, an ordered phase of type AuCu3I exists in the range from approximately 68 to 79 at.% 68 to 79 at.% Cu (Fig. 1, *a*).

Ordered alloys near the structure of AuCu with a long period (such as AuCu*II* [77] or in alloys Cu3Pd [76]) represent one of the interesting and promising classes of metal alloys (Fig. 1, *b*). They differ from ordinary ordered systems with a simple superstructure in that in alloys of this class the ordered arrangement of atoms is disrupted periodically or quasi-periodically by antiphase boundaries (APB) domains. Usually, in ordered alloys, APBs are energetically unprofitable; however, in systems with a long-period structure (LPS) APBs are the equilibrium elements of the structure. In the 'temperature−composition' phase diagrams, ordered alloys with a long period have well-defined stability regions.

If the antiphase shift occurs in the appendix (1/2, 1/2, 0), the resulting structure is of type *I*, in the appendix (1/2, 0, 1/2) and (0, 1/2, 1/2) — *II*a and *II*b, respectively. This is a single antiphase shift observed in the one-dimensional (1*D*) LPS. Single-stage DPS in stoichiometry of the type A3B (from which 2*D* LPS should be formed [79]) are constructed by translating the elementary cells $L1_2$ in appendix z and introducing regular (periodic) antiphase shifts postulated using APB with a short period, *e.g.*, $M = 1$ or 2, are usually found in alloys and are called $D0_{22}$ and $D0_{23}$ (Fig. 2). Structures with higher periods are called LPS [80].
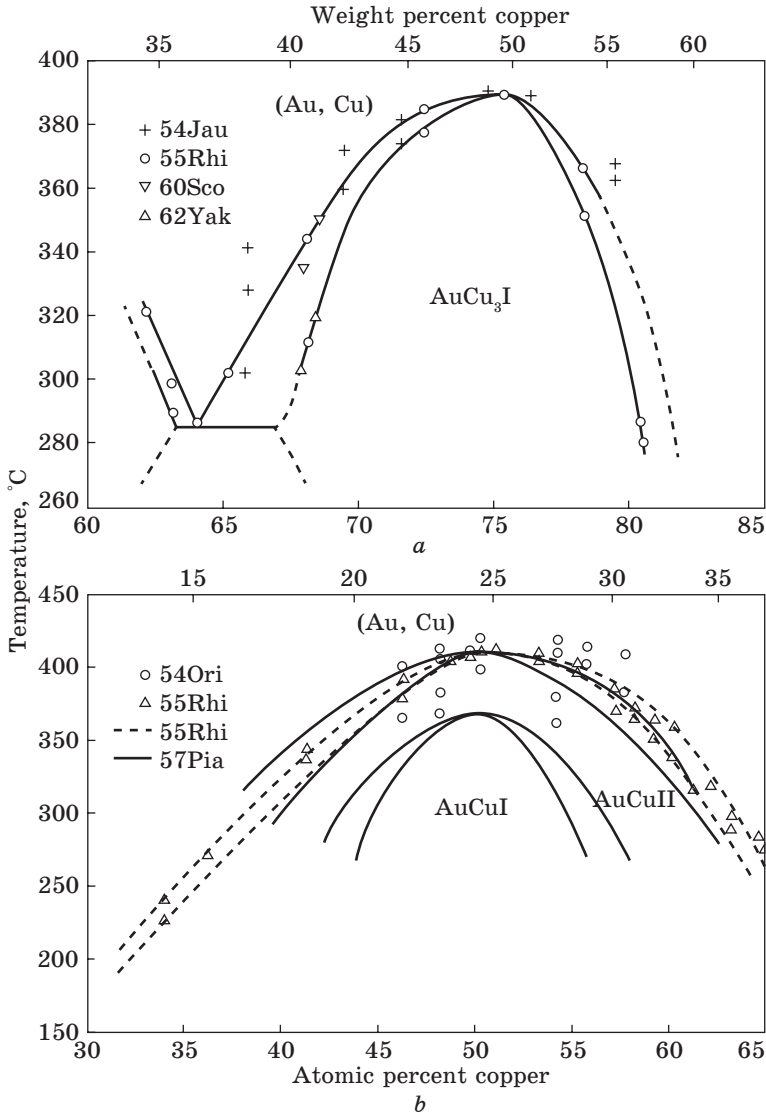
Fig. 1. Fragments of the phase state diagram Au–Cu [77]

The structure of AuCuII is an equilibrium, stable phase [81, 82], the period of which does not change during isothermal annealing. The two-dimensional LPS have two sets of APBs, one in each laying direction. In the second dimension, the distribution of type *II* APB is disrupted, which leads to two variants of type *II* APB, called *II*a and *II*b [83].

Although type *II* APBs were not observed in 1*D* LPS, they were observed in 2*D* LPS. Figure 3 shows the most interesting 2*D* types of LPS presented in Refs. [84] and [79] at finite temperatures. Following the no-
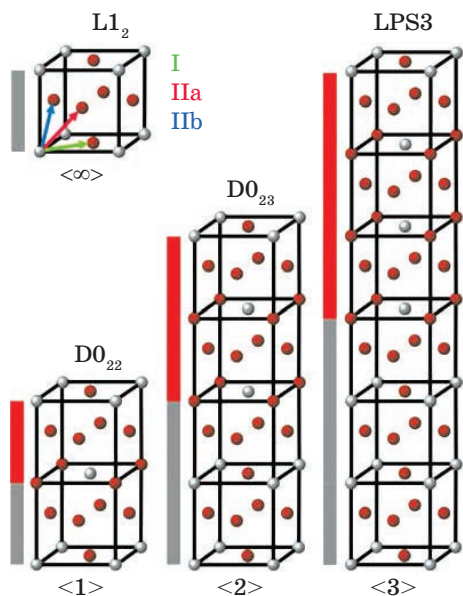
L1$_2$

LPS3

Fig. 2. Types of 1D LPS in A_3B alloy with a period $M = \langle 1 \rangle, \langle 2 \rangle, \langle 3 \rangle$ [76]

menclature introduced with their first appearance in the literature [85], we refer to a structure with type I APB in one direction and type IIa APB in the other ($M_I = M_{IIa} = 1$) (see Fig. 3). The study of alloys with 2D LPS has shown that it is not always a superposition of 1D LPS in two directions [86]. The APB between the two domains can be formed in several ways [87].

For the first time, the periodic structure was studied back in 1925 on epitaxial films [88]. Using x-ray images of the Cu–Au alloy, the authors established the occurrence of an ordered phase, as well as a change in electrical resistance depending on the composition. Later, it was possible to construct the first diagram of the states of the ordered phase in the Cu–Au system. In the ordered state, there are several reflexes on x-ray images, the intensity of which are determined by not only physical factors, conditions, and geometry of the survey, but also depend on the probability of filling with atoms of a certain type of the selected sublattice in the crystal; such reflexes are called superstructural [89].

Confirmation of the ordered structure in β-brass using radiographs was obtained in Ref. [90]. Later, in the 1950s, electron diffraction from antiphase domains (APD) was first observed [81], as well as superstructural reflexes of the structure CuAuII [91], and x-ray spectral analysis of superstructures was performed [92]. The formation of antiphase domains is energetically beneficial for the system since it is associated with a decrease in the symmetry of the ordered phase.

Further, in Ref. [85], the concentration dependence of the long-period structure for the Cu$_3$Pd alloy with a period of $M = 2$ and 3 was obtained, as well as temperature dependence [93]. The peculiarities of changes in interplanar distances from concentration were considered in Ref. [94]. At the same time, the dependence of the effect of deformation on the periodic structure and its electrical resistance was found in Ref. [95]. The drop effect in electrical resistance during heating was observed in Ref. [96].

The alloys of the Cu–Pt system form a continuous series of solid solutions. Under certain conditions of solid annealing, a whole range of or-
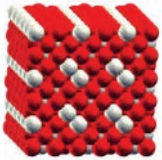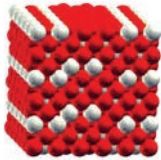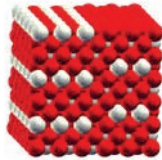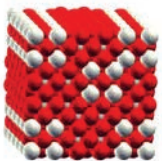
First six, simplest 2D LPSs at $x = 25\%$ Pd		
Crystal structure			
Name	$\langle 1_x 1_z \rangle$	$\langle 2_x 1_z \rangle$	$\langle 3_x 1_z \rangle$
Crystal structure			
Name	$\langle 2_x 2_z \rangle$	$\langle 3_x 2_z \rangle$	$\langle 3_x 3_z \rangle$
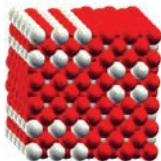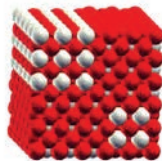
Fig. 3. Six minimum possible 2D LPS at $x = 25$ at.% Pd [76]

dered superstructures can occur in this system in certain concentration ranges at annealing temperatures below 645 °C and above 812 °C. It was experimentally found that the highest degree of order is achieved at platinum concentrations of 22.5, 50, 72.5, and 86 at.%, which corresponds to the superstructures $L1_2$ (Cu_3Pt), $L1_1$ (CuPt), $L1_3$ ($CuPt_3$), and the superstructure of the $CuPt_7$ composition. It should be noted that Cu−Pt alloys are the only dual system that transitions in an ordered state into several crystallographic structures from the disordered state of a regular solution based on the f.c.c. lattice. The alloy of the $CuPt_3$ composition is ordered into the $L1_2$ superstructure based on the symmetry of the f.c.c. lattice. The alloy of the equiatomic composition during the disorder−order transition is transformed from the crystallography of the f.c.c. lattice into the crystallography of the rhombohedral lattice corresponding to the superstructure with the angles α, β, and γ are different from $\pi/2$. Alloy Cu_3Pt is ordered as the $L1_2$ superstructure based on the f.c.c. lattice of a regular solid solution. The possibility of the existence of the most ordered phase of the alloy with 20% Pt was found, which corresponds to the Cu_4Pt phase. However, the type of superstructure has not been determined. In addition, the possibility of an ordered Cu_7Pt compound was predicted in the concentration range of 12.5% Pt. Thus, Cu−Pt alloys have many implementations of ordered superstructures in a wide range of component concentrations.

It should be noted the variety of structural transformations that occur in this system during the disorder−order phase transition, such as f.c.c.−f.c.c., and f.c.t.-rhombohedral structure. At the same time, the $L1_2$, $L1_0$, $L1_1$, $L1_3$ superstructures are implemented. However, to date, there is little information about the structural and phase transformations of
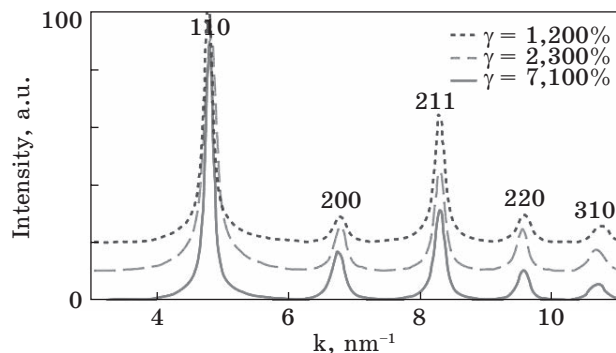
Fig. 4. Diffraction profiles of FeAl nanocrystalline regions after MPD for different deformation values [104]

this system depending on the concentration of components. Therefore, the study of possible types of superstructures implemented in the ordering depending on the concentration of components of alloys of the Cu–Pt system seems relevant.

As shown in the works [86, 97], dealing with the study of the formation and distribution of antiphase domains, the period of antiphase domains is a function of the concentration of Pd (for Cu_3Pd alloy). Also in 1957, in a paper [98] devoted to the study of the heat capacity of an ordered alloy, it was shown that the Debye temperature for the Cu3Au alloy increases in an ordered state. In theoretical work [99], the authors calculated the shape and amplitude of the distribution of antiphase domains for non-integer periods M, establishing six different distribution configurations and two directions of the antiphase structure. The ambiguities and limitations of the Bragg–Williams long-range order determination technique using the Paterson function were analysed in Ref. [100].

In the work [101], the authors studied periodic structures using x-ray analysis, they were able to measure the APB M period, and observe a change in the interplanar distance during ordering. The authors [102], when determining the degree of ordering of the periodic structure, proved that it increases in proportion to the increase in the period M. Using x-ray studies on AuCu films of the phase transition from AuCu*I* to AuCu*II*, the formation of coherent ordered lamellae was revealed, the structure of which differs from the matrix, which is accompanied by an increase in stresses and the formation of twins [103]. It was shown that the profiles of the curves of the x-ray spectra for the alloy FeAl in the nanocrystalline state are almost identical and do not depend on the magnitude of the introduced deformation and, accordingly, the grain size (Fig. 4) [104].

3. Metallographic Study of the Long-Range Ordered Alloys

Transmission electron microscopy is one of the main methods for studying alloys with periodic boundaries. This method makes it possible to determine the presence of a periodic structure by the appearance of splitting of superstructural reflexes in the diffraction pattern and by images of the periodic structures themselves.

Transmission electron microscopy is one of the main methods for studying alloys with periodic boundaries. This method makes it possible to determine the presence of a periodic structure by the appearance of splitting of superstructural reflexes in the diffraction pattern and by images of the periodic structures themselves.

For the first time in Refs. [82, 105], electron microscopic thermal antiphase boundaries and antiphase domains (APD) were observed in the atomically ordered alloy Cu_3Au in the early 1960s (Fig. 5).

APB can be observed because of the appearance of additional diffraction contrast in the form of dark lines or the form of pairs of stripes. At the same time, the authors of the papers studied the long-periodic atomic ordered structure (Fig. 6) [83, 106].

In Ref. [107], it was shown for the first time that at least three superstructural beams must be used to form a 'direct resolution' image of antiphase domains (Fig. 7). In addition, as in the case of AuCu*II*, the authors [108] showed that the APB period in Ag_3Mg remains constant on both dark-field and light-field images (Fig. 8).

In Ref. [109], periodic structures on films of atomically ordered Cu−Pd alloys were studied, and, for the first time, a step-by-step ordering of a long-period structure from near to far order was shown, as the diffraction pattern changes depending on the content of Pd and superstructural reflexes are redistributed (split).

In Ref. [110, 111], the case of the formation of a structure with a long-range order was considered, when the sublattices in different parts of the crystal do not coincide, in this case, APDs are formed. The authors of a series of theoretical papers on the study of one-dimensional antiphase domain structures improved the model for non-integer APBs by disordering the structure consisting of two types of APBs with a period of M and $M + 1$ and derived the corresponding step function. The scheme of AuCu*I* phase growth from the AuCu*II* phase is clearly shown in Ref. [100] (Fig. 9).

In Ref. [112], the high thermal stability of periodic structures was noted, which is important from the point of view of the structural properties of atomically ordered alloys. Using the example of diffraction patterns, the authors of [113] developed and proved a theory that helps to explain the initial stage of ordering and the transition from near to far order.

In Ref. [114], the direct resolution of an atomically ordered structure was published for the first time (Fig. 10). The authors also showed that the order−disorder transition occurs by two mechanisms (heterogeneous and homogeneous): the creation of an ordered phase on APB and the mechanism of the origin and growth of a disordered phase inside ordered domains.

Two groups of long-period states have been experimentally discovered: in the first group, the stabilization of atomic ordering is determined by relaxation processes, and in the second, the competing interaction in different coordination spheres plays a decisive role. The initial stage of order
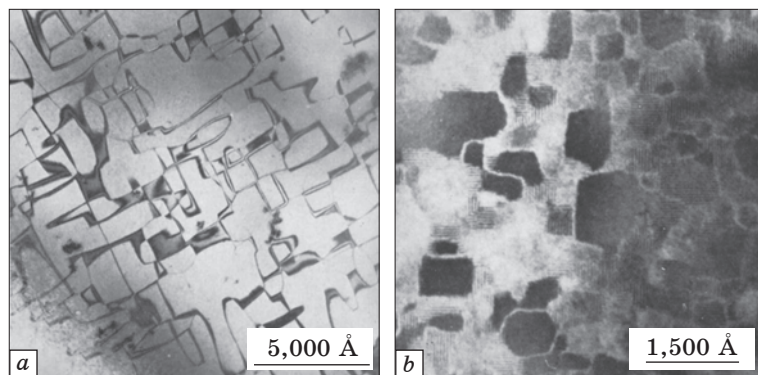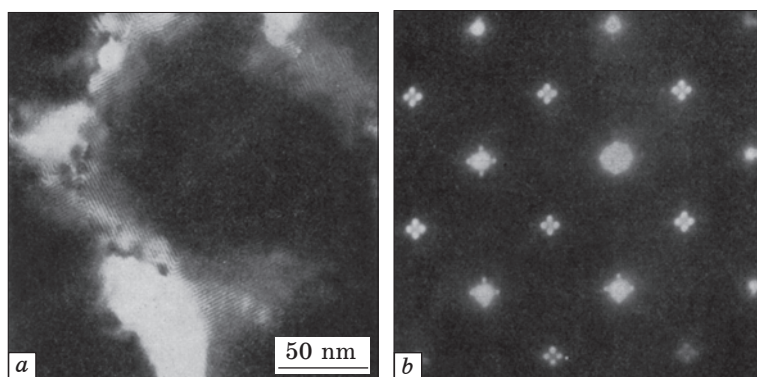
Fig. 5. (*a*) Thermal APB and (*b*) antiphase domains in Cu$_3$Al [105]

Fig. 6. (*a*) Antiphase domain structure in Au-Cu*II* and (*b*) corresponding electronogram [106]

was also studied in Ref. [79], where the authors were able to determine the exact conditions for forming a short-range order for Cu–Pd alloys.

The authors [115] for the first time established the presence of localized antiphase shifts, constructed the temperature dependence of the average size of antiphase domains, and explained the nature of APB in a one-dimensional periodic superstructure, dividing them into 'wavelike' and 'diffuse'. Thanks to the Fourier transform, they very clearly showed the formation of APB using transmission electron microscopy (TEM). The clearest APB was obtained for the alloy with 25.2 at.% Pd (Fig. 8), which was agreed upon in the works [85].

To obtain a direct image of periodic boundaries in an alloy, two conditions must be satisfied: a sufficiently high resolution of the TEM and a high degree of control over the crystallographic orientation of the samples. The second condition is fulfilled in the presence of a special goniometric table, but its installation on most modern microscopes entails a decrease in resolution. In this regard, such studies were previously usually carried out using electron microscopes on specially prepared epitaxial films having the necessary orientation of the crystallographic axes relative to the surface of the film, which eliminates the need for a goniometric table.
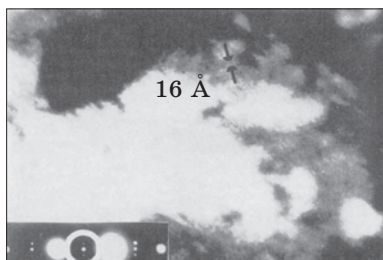
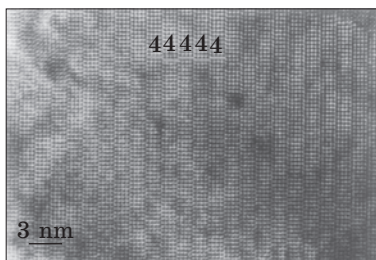*Fig. 7.* Antiphase domain interference scheme in Ag_3Mg [107]

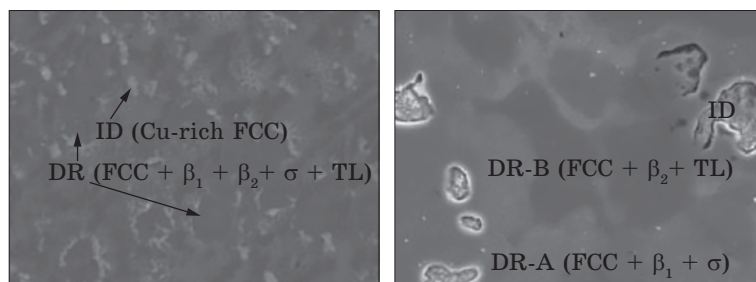*Fig. 8.* The direct resolution of $1D$ LPS 4 in Cu−25 at.% Pd annealed at 424 ºC [115]

Fig. 9. The microstructure of the high-entropy alloy $Al_{0.5}CoCrCuFeNiTi_x$, obtained by the SEM method, with Ti content in the alloy $x = 1.2$. TL is the Ti_2Ni phase, σ is the CoCr phase, DR is the dendritic region, and ID is the interdendritic region [131]

The work [116] shows the evolution of the structure of atomically ordered alloys with a lattice of type $L1_2$ under the influence of MPD and the stages of destruction of the long-period structure because of the action of MPD. In Ref. [117], the dependence of the degree of order, the size of the antiphase domains, moreover the effect of temperature and annealing time on these parameters were investigated. It turned out that the greater the micro deformation of the crystal lattice, the lower the degree of order, and at the maximum degree of order, the distortions are close to zero. It can be concluded that a long-range atomic order creation is possible only in the case of a small size of antiphase domains [118−130].

In Ref. [131], the microstructure and properties of high-entropy $Al_{0.5}CoCrCuFeNiTi_x$ alloys with different Tix content ($x = 0−2$) were investigated and some interesting facts were established. For example, with a low Ti content, the alloys had mainly an f.c.c.-solid solution phase, however, already with a titanium content of $x = 0.4$, the two b.c.c. phases β_1 and β_2 appeared, and then β1 phase became ordered at $x = 1.4$. As the Ti content in the alloy increased, nanowires enriched in copper were segregated in the interdendritic region (Fig. 9). Chemical (x-ray EMF) and x-ray diffractometric analysis showed that the CoCr and Ti_2Ni phases were formed in the dendritic region at $x = 0.8−1.2$ and $x = 1.2−2.0$, respectively.
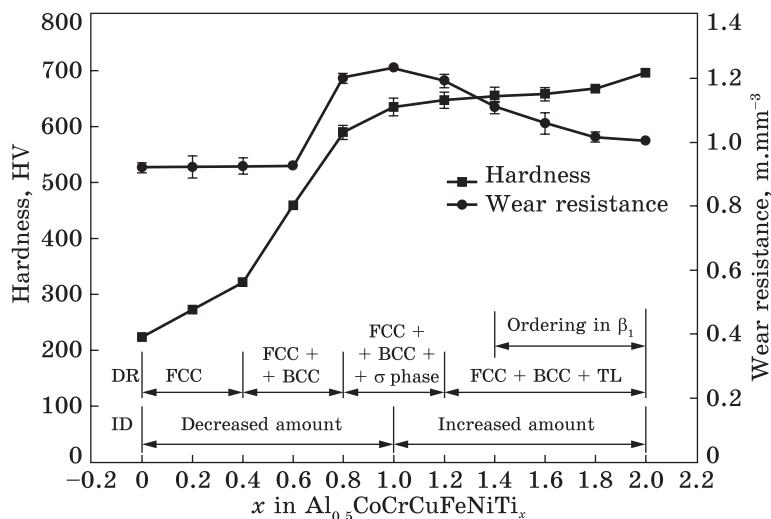
Fig. 10. The dependence of hardness (according to Vickers) and wear resistance on the Ti content in the high-entropy alloy $Al_{0.5}CoCrCu$ $FeNiTi_x$. TL is the Ti_2Ni phase, σ is the CoCr phase, DR is the dendritic region, and ID is the interdendritic region [131]

The hardness values of the high-entropy alloy $Al_{0.5}CoCrCuFeNiTi_x$ increased with an increase in the Ti content and the number of phases of b.c.c., Ti_2Ni and CoCr in the dendritic region of the alloy (Fig. 10). The wear resistance of the alloy was also measured, which showed that at a low Ti content, the wear resistance remained at the same level as that of the original alloy ($Al_{0.5}CoCrCuFeNi$) without Ti content, however, at $x = 0.6-1.0$, the values of the wear resistance increased and reached their maximum at $x = 1.0$. Thus, the best combination of hardness and wear resistance in $Al_{0.5}CoCrCuFeNiTi_x$ alloys was obtained with Ti content in the alloy $x = 0.8-1.2$, that is, with the formation of the σ-phase CoCr [131].

Similar experiments with varying the content of another element (V) in the high-entropy alloy $Al_{0.5}CoCrCuFeNi$ were described in the article [132]. With a small addition of vanadium $Al_{0.5}CoCrCuFeNiV_x$, the alloys had a simple f.c.c. solid solution phase. As the vanadium content increased to $x = 0.4$, a b.c.c. phase appeared in the dendritic region because of the assumed spinodal decomposition. With an increase in the V content from $x = 0.4$ to 1, the volume fraction of the b.c.c. phase increased. When the vanadium content in the alloy reached $x = 1$, the dendritic f.c.c. structure was completely replaced by a b.c.c.-dendritic one. Then, with an increase of $x = 1.2$ to 2, a needle phase σ was formed in the spinodal decomposition process (Fig. 11) [132].

4. Nanostructural State in Ordered Alloys

Metals and alloys with nanoscale structural elements are weakly resistant to external influences (temperature, load, composition changes, alloying, *etc.*). In addition, atomically ordered alloys in the nanostructured state
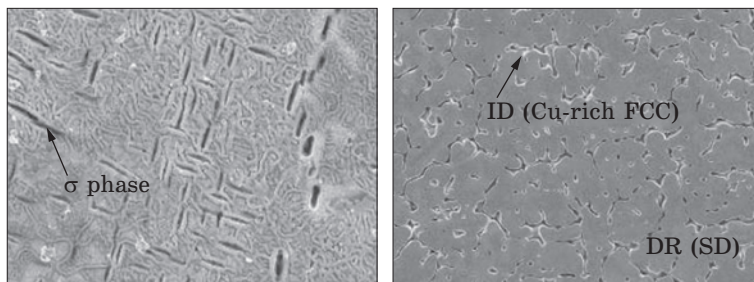
Fig. 11. The microstructure obtained by the SEM method of a high-entropy alloy $Al_{0.5}CoCrCuFeNiV_x$ with V content in the alloy $x = 1.0$. SD is spinodal decay, σ is a needle phase enriched in V, DR is a dendritic region, and ID is an interdendritic region [132]

have good magnetic properties, as described in [103]. MPD is one of the principal methods that ensure the achievement of large accumulated deformations in materials with values of true logarithmic deformation equal to 10 or more, without destroying samples. MPD includes high-pressure torsion (HPT) and equal-channel angular compression [133–137]. When deformed by torsion under high pressure, the obtained samples have the shape of discs with a diameter of 10–20 mm and a thickness of 0.2–1.5 mm, clamped by strikers on both sides. Rotation of one of the strikers due to friction forces ensures shear deformation of the sample by the strikers under the applied pressure of several GPa. Therefore, despite the large values of the true deformation, the sample does not collapse. As research shows [138], during the implementation of this scheme of intensive plastic deformation, not only on the periphery of the disks but also in their central part, after several revolutions, the structure is sharply crushed and becomes almost homogeneous along the radius of the samples. This is confirmed by the convergence of microhardness values at different points of the sample.

A comparatively promising method of deformation formation of nanostructures in bulk samples is comprehensive forging or pressing, when compression deformation operations are repeated many times with a sequential change of the axis of the applied deforming force. It also allows you to preserve the volume, shape, and dimensions of the workpiece, ensuring its intense hot deformation, which is usually accompanied by dynamic processes of return, polygonization, and recrystallization, which contribute to deformation even in sufficiently fragile materials and with relatively small specific loads on the tool [139–145].

Systematizing the known data, it can be firmly concluded that nanostructured metals, their alloys, compounds, and composites studied under different schemes of mechanical tests (stretching, compression, bending, torsion) demonstrate significantly higher (several times) values of tensile

strength and yield strength. However, in some cases they have noticeably less pronounced deformation hardening at the plastic deformation stage during testing and, as a result, a smaller increase in hardening and lower plasticity. These circumstances, as well as violations of the Hall–Petch ratio, are obviously due to the inclusion in nanostructured materials of new deformation mechanisms based on grain boundary non-crystallographic shear or rotational slippage, already at relatively low or even at any temperatures competing with the action of standard crystallographic intragrain dislocation sliding and twinning or replacing and ignoring them [146].

The special role of the state of the boundaries of nanograins is confirmed by experiments with such short-term low-temperature annealing, as a result of which the average size of nanograins practically does not grow, but there is some return of the defective structure and an increase in its perfection, and, above all, at the grain boundaries. After such treatments, the mechanical deformation behaviour of nanostructured materials radically changes: high yield strength is achieved, and a significantly greater elongation is fixed. It should be noted that many nanostructured materials, in addition, exhibit high-temperature superplasticity (up to 1000%) because of grain boundary slippage at higher deformation rates and lower temperatures than conventional polycrystalline alloys of the same compositions in the superplasticity mode. Paper [147] shows an increase in the characteristics of cyclic loading and wear resistance of materials in the nanostructured state. In Ref. [148], it was shown that the peaks of the x-ray spectra begin to smooth out with a decrease in grain size to the nanostructural state. The typical structure of equiaxed grains in the nanostructured state obtained using MPD by the HPT method is shown in Fig. 12 [138].

High tensile strain leads to intercrystalline fracture regardless of grain size (in the range from 10 to 65 nm) (Fig. 13) [149]. The electron microscopic image of direct atomic resolution shows that the origin and propagation of the crack occur along the double boundary (Fig. 13, *b*).

To determine the quantitative parameters of the grain size of crystallites and elastic microdistortions of the crystal lattice of the alloy in the nanostructural state after MPD, an analysis of the physical profile of x-ray peaks is used. At the same time, if the effect of MPD has been studied in detail on many metals and model alloys, such studies on atomically ordered alloys are practically absent.

50 nm
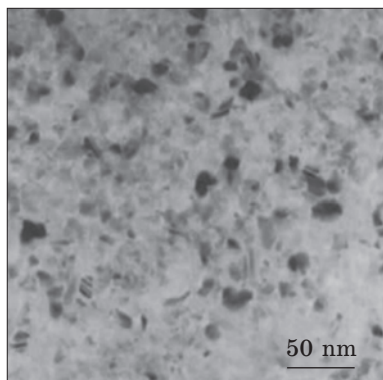
Fig. 12. Light-field TEM image of equiaxed nanocrystalline Cu grains [138]
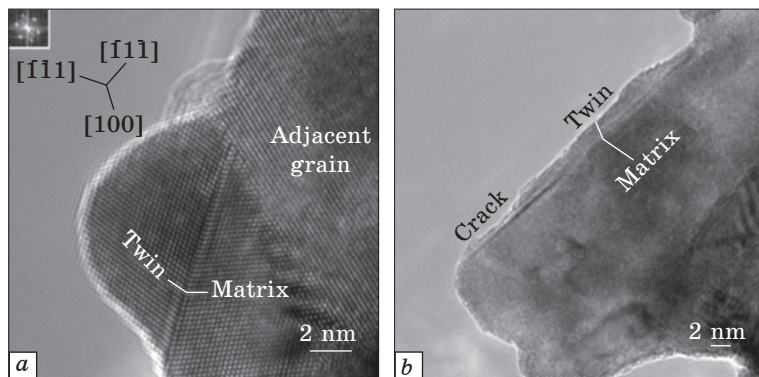
Fig. 13. Light-field TEM image of intercrystalline grain fracture during deformation in the nanostructural state [149]

The ordered state in nanostructures has also been observed experimentally and studied theoretically in a series of works devoted to the low-dimensional (quasi-two-dimensional) structures, first of all, based on graphene and graphene-related systems [150–164].

5. Change in Electrical Resistance during Ordering

Several works are devoted to the influence of the ordering of the Cu_3Pd alloys on electrical resistance, as well as the dependence of electrical resistance on the structure and phase state of the alloy.

Knowing the wave properties of conduction electrons, predicting the change in resistance during ordering is possible. So, suppose the crystal lattice of a metal or alloy contains any distortions that lead to a violation of the periodicity of the potential. In that case, the scattering of electronic waves appears, causing an increase in electrical resistance.

At concentrations corresponding to the transition from the disordered to the ordered phase, characteristic features should be observed on the curve $p_0(c_A)$ for alloys annealed at the same temperature. Since, during phase transitions of the second kind, the degree of long-range order changes continuously with temperature, it must also change with the composition of alloys annealed at the same temperature. Therefore, the electrical resistance, in this case, should also change continuously, but at concentrations of $c_A = c_0$, the curve of dependence of electrical resistance on the composition should have fractures. If the order–disorder phase transition is a phase transition of the first kind, then, the degree of long-range order changes abruptly, and, during the transition to an ordered state at concentrations $c_A = c_0$, the electrical resistance of the alloy should decrease abruptly.

Additional features of the concentration dependence of the residual electrical resistance of the alloy appear if the electron energy spectrum changes significantly when the alloy composition changes in a certain con-

centration range. Such a change in the energy spectrum occurs, *e.g.*, in alloys of transition metals with non-transition metals. In this case (using the terms of the one-electron approximation), in a certain concentration range in alloys, there is an unfilled d-band of the electron energy spectrum with a significantly higher density of electronic levels than in the *s*-band. The probability of scattering of *s*-electrons on inhomogeneities of the crystal lattice increases remarkably, because there is a possibility of transitions not only to *s*-levels but also to unfilled *d*-levels. By this, the number of quantum transitions of conduction electrons per unit of time, which determines the value of electrical resistivity, becomes greater. As a result, the residual electrical resistance of alloys in the concentration range corresponding to unfilled *d*-levels increases significantly.

It is important to note that in general, the alloys A_3B may differ materially from another T_c and the kinetics of atomic ordering, for example, in the alloy Cu_3Au, but slow in Cu_3Pd. With increasing temperature, as already mentioned, additional distortions of the crystal lattice of the alloy occur, correlated with thermal fluctuations. Therefore, even if the distribution of atoms at the sites of the crystal lattice of the alloy does not change with a temperature change, the electrical resistance increases with an increase in temperature.

Further heating causes an increase in electrical resistivity, which is associated with the processes of disordering occurring in the samples. At a temperature of 730 °C, the electrical resistance of all the studied samples becomes approximately the same regardless of the initial state (*i.e.*, the state of the material is approaching equilibrium). Studying the effect of the order–disorder phase transition on the change in the thermal resistance coefficient, the authors [78] proved that the transition from a disordered state to a long-range order and vice versa is carried out through a structure with a short-range atomic order (Fig. 14). In addition, Fig. 14 shows how the resistance and phase transformations change depending on the heating rate, it can be seen that the minimum speed allows you to obtain a lower resistance, and therefore a higher degree of long-range order.

This subsection very briefly describes the effect of ordering in the electrical resistance of the cubic-lattice-based alloys. A series of another works dealing with response of ordering in the residual resistivity (for both cubic- and non-cubic-lattice-based alloys) are analysed in reviews [50, 53] and references therein as well as in articles [165–174].

6. Kinetics of the Formation of Periodic Superstructures

For the first time, the principles of the formation of long-period superstructures were set out in the model of spatial correlation of electrons described in Ref. [175], where the main idea is the energy benefit of creating APB with lattice distortions, *i.e.*, the direct relationship between the
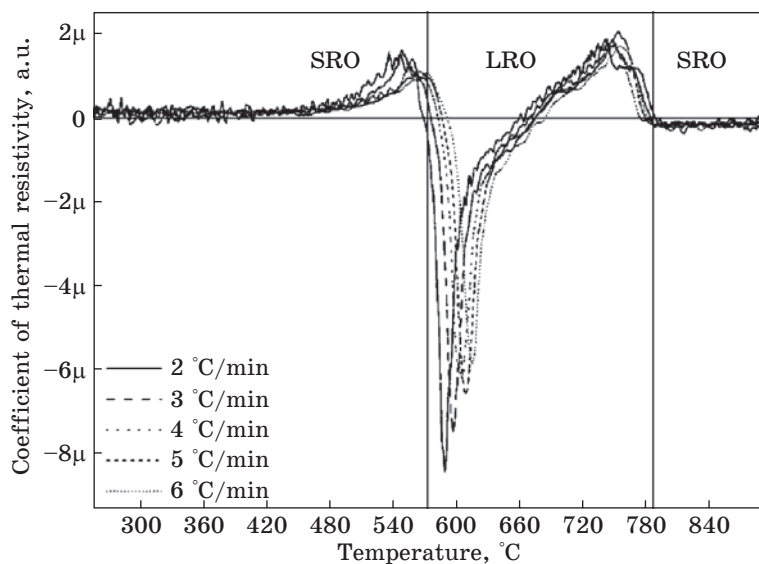
Fig. 14. The coefficient of thermal resistivity is plotted as a function of temperature for different heating rates of $Ni_2(Cr_{0.5}Mo_{0.5})$ hardened from 1423 K [78]

concentration of valence electrons and the density of APB. In the electronic theory proposed by the authors [83, 176], the main principle is also the reduction of the systems' energy. The energy of the alloys' electronic system decreases, if the Fermi surface comes into contact with the boundaries of the Brillouin zone [177]. Since the appearance of periodic boundaries in the alloy is accompanied by the division of the Brillouin zone, the Fermi surface can come into contact with the zone boundaries [178]. However, the structure of an alloy with periodic boundaries will be stable only if, due to the contact of the Fermi surface with the boundaries of the Brillouin zone, the energy of the alloy decreases so much that it will more than compensate for the additional energy required to create a large number of periodic APBs [179]. Thus, by controlling these two energy parameters, it is possible to suppress or make a structure with APB, as well as change the size of the *M* period.

Each temperature corresponds to a certain equilibrium value of the parameters characterizing the far and near order. However, these values are not set instantly, but over time by the processes of redistribution of atoms at the sites of the crystal lattice. Therefore, some physical quantity *Q*, depending on the ordering of the alloy, will take equilibrium value Q_p corresponding to a given temperature, not immediately, but after infinitely long annealing at this temperature.

In Ref. [180], a strong influence of the electronic distribution on the thermodynamic properties associated with the phase transition was shown.

The kinetics of ordering in alloy 3 has been studied in the most detail, where the order–disorder transition is a phase transition of the first kind. The Cu_3Au and Cu_3Pd alloys are stoichiometrically the same. If such an alloy is annealed after a long time at a temperature higher than the ordering temperature of T_0 (*i.e.*, being in a disordered state), it cools quickly to a temperature of $T < T_0$. Then, the process of establishing an equilibrium state with a long-range order will occur in two stages. First, at certain points of the crystal (where the short-range order was greatest), centres of a newly ordered phase are formed and grow into contact, in which, at this first stage, the long-range order parameter close to equilibrium is established.

Since all the sites of the crystal lattice were equivalent in the disordered state, the distribution of copper and gold atoms along the sites of the initial f.c.c. lattice may be different in the various ordered regions that arose, called domains. The second, which proceeds more slowly in the process of establishing an equilibrium-ordered state in the alloy, is the growth of some domains at the expense of others and the transition as a result of this alloy to a state with homogeneous ordering. By the presence of such two stages of establishing order, the ordering process can be approximately characterized by two different relaxation times. With rapid heating of a previously ordered alloy to a temperature higher than the ordering temperature and isothermal exposure at this temperature, the disordering process has only one stage. Indeed, in this case, even an alloy, that had a domain structure before heating, after the disappearance of order in each domain becomes homogeneous (disordered), and no process of combining different regions is needed to achieve equilibrium. The alloy transition to an ordered state, as already noted, is associated with the diffusion processes of redistribution of atoms at the sites of the crystal lattice [181]. These processes are characterized by certain activation energies and become extremely slow at low temperatures. As the temperature of the isothermal exposure increases, the relaxation time decreases rapidly at first. However, as this temperature approaches the ordering temperature, in addition to the diffusion rate, another factor becomes significant, because the ordering process slows down with a decrease in the difference in free energies of the ordered and disordered phases corresponding to a given temperature. At temperatures close to ordering, this difference is tiny, and therefore, despite the significant diffusion rate, ordering occurs slowly, *i.e.*, the relaxation time again reaches large values. Lowering the temperature in this temperature range accelerates the ordering process. Thus, the relaxation time will decrease with a deviation in any direction from the ordering temperature.

Consequently, there is a minimum on the curves of the temperature dependence of relaxation times for various values. It should be noted that, if the relaxation process takes place over a considerable time, then, the temperature dependences of the different properties of the alloy, measured res-

pectively during heating or cooling of the sample, will differ, *i.e.*, hysteresis-type curves should be obtained. With a decrease in the rate of heating and cooling, hysteresis phenomena should be manifested to a lesser extent.

The presence of a domain structure in an ordered alloy could also explain that the time of bringing the alloy from an unordered state to an equilibrium ordered one ($\approx$70 h) was significantly longer than the time of bringing the alloy into an unordered state from an ordered one ($\approx$15 min), because in the latter case, as already indicated, there is no second, slow-flowing stage of the process. The regions of the ordered phase formed at the first stage of ordering are tiny and do not have a noticeable effect on the electrical resistance of the alloy, nor do they cause the appearance of superstructural lines. The course of the ordering process at this stage, however, can be investigated by studying the heat capacity of the alloy, which is sensitive to the redistribution of atoms in small volumes having linear dimensions of the order of several atomic distances. The strong temperature dependence of the relaxation process rate is because a change in the degree of long-range order, which determines the magnitude of electrical resistance, occurs using a diffusion mechanism. As a result, the rate of change in the order parameter is greater the higher the concentration of vacancies at the sites of the crystal lattice of the alloy (holes) and their mobility, which, as is known, increase rapidly with increasing temperature. The observed significant decrease in electrical resistance is due to the occurrence of a large number of equilibrium vacancies at the lattice sites at these temperatures. As the temperature increases, the equilibrium value decreases, and as a result, the resistance, after passing through the minimum, begins to rise again. By studying the kinetics of ordering in the alloy Cu_3Au at low temperatures, it could be established that the activation energy for the movement of vacancies in this alloy is approximately 0.9 eV.

7. Deformation Mechanisms in Superstructures

Numerous works have been devoted to the study of dislocations in atomically ordered alloys and, the study of the effect of deformation on the mechanical properties of the periodic structure [182]. The deformation effect over a wide temperature range leads to the generation of deformation antiphase boundaries, contributes to a decrease in the average size of antiphase domains, and, accordingly, leads to an increase in the density of antiphase boundaries, which stimulates the emergence of additional contributions to deformation resistance. The stages of deformation, changes in microstructure, and grain size are also studied in detail in Ref. [183]. It was shown in Ref. [184] that deformation processes can positively affect the ordering in the alloy, delaying recrystallization, and making it possible to undergo atomic ordering. The peculiarity of ordering systems is that plastic deformation is associated with over-dislocations. In general,

an over-dislocation is a complex containing single split dislocations, APB bands, and packaging defects of various types [185].

In Ref. [185], an ideal deformation scheme is presented, based on the assumption that the periodic anti-phase domain structure is also perfect. Only in this case, the crystal structure is restored during the passage of the dislocation complex. However, an analysis of the literature data shows that the periodic domain structure is never ideal. The period of almost all such alloys, when accurately measured, turns out to be either non-integer or odd, which indicates the mixing of domains of different sizes. For the Cu_3Pd alloy with a period of 7 parameters, the alternation of atomic boundaries, according to Ref. [186], can be represented as 34343343434434. In all alloys with a periodic structure, in addition to periodic ones, there are thermal boundaries, which, unlike periodic boundaries, are located arbitrarily, as well as the boundaries of domains.

The introduction of not one, but many 'superfluous' boundaries into the structure or the mixing of domains of equal size will lead to the formation of numerous sections of the antiphase surface during deformation. As a result, the long-range order in the current sliding plane will be disrupted. In this case, microscopic sections of the antiphase surface alternate with sections in which the long-range order is preserved. Such defective planes were called planes with a broken long-range order. Planes with a broken long-range order continue to exist even after passing through several dislocations. The formation of special defects at the initial stages of deformation, planes with a disturbed long-range order, can explain all the experimental facts. Dislocations, except the first ones, are forced to move in planes with a broken long-range order. At the same time, single dislocations no longer leave behind a high-energy defect, and therefore the movement of paired or other complex dislocations now has no advantages, that is, the incentive to combine dislocations into paired or complex dislocations disappears.

For this reason, mainly single dislocations are observed electron microscopically in deformed alloys with a periodic ordered structure. It also becomes clear that there is no significant difference in the dislocation structure of alloys with different period values for layered and columnar structures: a rapid violation of the long-range order in the sliding planes should occur in any alloy with a sufficiently high density of APB, including in periodicity. The area of the sections that make up the plane with a disturbed long-range order should be larger the more dislocations and disturbances in the considered sliding plane. However, a violation of the long-range order probably does not occur until complete disordering for the following reasons. After the long-range order in the sliding plane was violated, but there were still areas with correct connections (characteristic of an ordered state), it became equally difficult for both single and paired dislocations to move. For further movement of dislocations in this plane,

a significant increase in voltage would be required, therefore, it becomes advantageous to activate another sliding plane, and this process is repeated repeatedly.

In the studied copper–palladium alloys, such partial dislocations, as we have seen, can move only in planes with a disturbed long-range order. Although these planes are located close to each other, they do not form in a row in each sliding plane belonging to a pack of parallel planes. Therefore, the pole twinning mechanism does not work, and extended packaging defects are often found in copper–palladium alloys, but microtwinning is never observed. In some cases, planes with a disturbed long-range order can produce diffraction-banded contrast in an electron-microscopic image, the analysis of which indicates that it is due to a disturbed long-range order:

• the planes of occurrence of defects causing banded contrast are planes of type {111}, that is, those in which planes with a disturbed long-range order should occur during deformation;

• banded contrast is observed only if the foils of alloys with periodic boundaries have been deformed;

• banded contrast is not detected in any alloy if a disordered state is fixed in it by quenching;

• if the alloy samples in which the contrast under discussion is observed are briefly heated to a high-temperature T, but such that $T < T_c$, then the contrast disappears; this is explained by the diffusive restoration of order in the sliding planes, which can be conditionally called 'healing' of planes with a disturbed long-range order.

Moreover, a weakening of the striped contrast was observed until its disappearance and during long-term storage of deformed foils (at room temperature). What is common for Cu–Pd and Cu–Au alloys is that their lattice parameters change when they are ordered. Moreover, their elementary cell changes, first it becomes tetragonal, and then orthorhombic. In the alloy Cu_3Au (31.6 at.% Au), the crystal lattice parameter changes very little during ordering, the difference is only a few thousandths of Å [187]. With such a difference in the parameters of the ordered and disordered phases, the occurrence of a defect in the form of a plane with a disturbed long-range order does not lead to a significant displacement of one part of the crystal relative to the other. Hence, the mechanism of plastic deformation of real alloys with a periodic antiphase structure is determined by the formation of special defects already at the initial stages of deformation, namely, planes with a disturbed long-range order. Therefore, the deformation of alloys passes uniformly along many sliding planes and is carried out not only by paired, but by split and single dislocations. Shockley dislocations become possible with the appearance of extended packaging defects.

There is particular importance of the dynamic and post-dynamic recrystallization processes, which occur both during deformation at room temperature and at liquid nitrogen temperature. Thus, in [188], a scheme
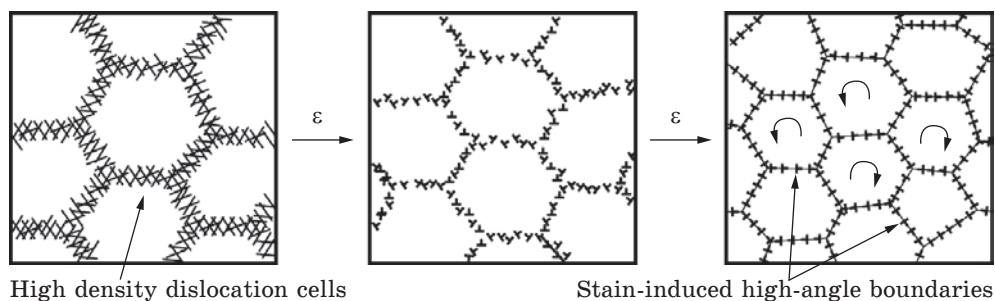
High density dislocation cells   Stain-induced high-angle boundaries

Fig. 15. The coefficient of thermal resistivity vs. the temperature for different heating rates of $Ni_2(Cr_{0.5}Mo_{0.5})$ hardened from 1423 K [78]

for the formation of high-angle boundaries during deformation is shown in detail (Fig. 15).

8. Conclusions

One of the fundamental and practically oriented tasks of condensed matter physics and physical metrology is the development of the physical foundations for the creation of new metal materials and technologies for their production with a complex of necessary physical, mechanical, and operational characteristics, structural and functional. As is known, the mechanical properties of materials significantly depend on their chemical composition and features of the crystal-structural state, such as structural type, grain sizes, types of their boundaries, number and size distribution, and volume of inclusions of excess phases, density, dislocation substructure, *etc.* In the last two to three decades, it has been established that a significant improvement of the physicomechanical properties of metallic materials can be achieved due to the ultrafine-grained structure (submicron and nanocrystalline and nanophase). Various methods of its formation have been developed, including those based on thermal (including rapid quenching from a melt) and thermomechanical external influences, the use of various combinations of large deformations, and annealing. They make it possible to design, using mechanical and thermoinduced processes, optimal structural states and control some properties of such materials within a wide range.

REFERENCES

1. C.-C. Tung, J.-W. Yeh, T.-T. Shun, S.-K. Chen, Y.-S. Huang, and H.-C. Chen, On the elemental effect of AlCoCrCuFeNi high-entropy alloy system, *Mat. Letters*, **61**: 1–5 (2007); https://doi.org/10.1016/j.matlet.2006.03.140
2. B.S. Li, Y.P. Wang, M.X. Ren, C. Yang, and H.Z. Fu, Effects of Mn, Ti and V on the microstructure and properties of AlCrFeCoNiCu high entropy alloy, *Mater. Sci. Eng. A*, **498**, Nos. 1–2: 482–486 (2008); https://doi.org/10.1016/j.msea.2008.08.025
3. B. Jang, S. Riemer, and G.M. Pastor, Chiral magnetic interactions in small fe clusters triggered by symmetry-breaking adatoms, *Symmetry*, **15**, No. 2: 397 (2023);

https://doi.org/10.3390/sym15020397

4. Z. Liu, S. Guo, X. Liu, J. Ye, Y. Yang, X.-L. Wang, L. Yang, K. An, and C.T. Liu, Micro-mechanical characterization of casting-induced inhomogeneity in an $Al_{0.8}$CoCrCuFeNi high-entropy alloy, *Scripta Mater.*, **64**: 868–871 (2011); https://doi.org/10.1016/j.scriptamat.2011.01.020

5. I.E. Volokitina, A.V. Volokitin, and E.A. Panin, Martensitic transformations in stainless steels, *Prog. Phys. Met.*, **23**, No. 4: 684–728 (2022); https://doi.org/10.15407/ufm.23.04.684

6. I.E. Volokitina, A.V. Volokitin, A. Bychkov, and A. Kolesnikov, Natural aging of aluminum alloy 2024 after severe plastic deformation, *Metallography, Micro-structure, and Analysis*, **12**, No. 3: 564–566 (2023); https://doi.org/10.1007/s13632-023-00966-y

7. N. Zhangabay, I. Baidilla, A. Tagybayev, U. Suleimenov, Z. Kurganbekov, M. Kambarov, A. Kolesnikov, G. Ibraimbayeva, K. Abshenov, I. Volokitina, B. Nsanbayev, Y. Anarbayev, and P. Kozlov, Thermophysical indicators of elaborated sandwich cladding constructions with heat-reflective coverings and air gaps, *Case Studies Construct. Mater.*, **18**: e02161 (2023); https://doi.org/10.1016/j.cscm.2023.e02161

8. Z. Hu, Y. Zhan, G. Zhang, J. She, and C. Li, Effect of rare earth Y addition on the microstructure and mechanical properties of high entropy AlCoCrCu-NiTi alloys, *Materials and Design*, **31**: 1599–1602 (2010); https://doi.org/10.1016/j.matdes.2009.09.016

9. M.-I. Lin, M.-H. Tsai, W.-J. Shen, and J.-W. Yeh, Evolution of structure and properties of multi-component $(AlCrTaTiZr)O_x$ films, *Thin Solid Films*, **518**: 2732–2737 (2010); https://doi.org/10.1016/j.tsf.2009.10.142

10. I.E. Volokitina, Structural and phase transformations in alloys under the severe plastic deformation, *Prog. Phys. Met.*, **24**: No. 3: 593–622 (2023); https://doi.org/10.15407/ufm.24.03.593

11. S. Singh, N. Wanderka, K. Kiefer, K. Siemensmeyer, and J. Banhart, Effect of decomposition of the Cr–Fe–Co rich phase of AlCoCrCuFeNi high entropy alloy on magnetic properties, *Ultramicroscopy*, **111**: 619–622 (2011); https://doi.org/10.1016/j.ultramic.2010.12.001

12. O.N. Senkov, J.M. Scott, S.V. Senkova, D.B. Miracle, and C.F. Woodward, Microstructure and room temperature properties of a high-entropy TaNbHfZrTi alloy, *J. Alloys and Compounds*, **509**: 6043–6048 (2011); https://doi.org/10.1016/j.jallcom.2011.02.171

13. X. Ye, M. Ma, Y. Cao, W. Liu, X. Ye, and Y. Gu, The property research on high-entropy alloy alxfeconicucr coating by laser cladding, *Physics Procedia*, **12**: 303–312 (2011); https://doi.org/10.1016/j.phpro.2011.03.039

14. C.-M. Lin and H.-L. Tsai, Evolution of microstructure, hardness, and corrosion properties of high-entropy $Al_{0.5}$CoCrFeNi alloy, *Intermetallics*, **19**: 288–294 (2011); https://doi.org/10.1016/j.intermet.2010.10.008

15. K.G. Pradeep, N. Wanderka, P. Choi, J. Banhart, B.S. Murty, and D. Raabe, Atomic-scale compositional characterization of a nanocrystalline AlCrCuFeNiZn high-entropy alloy using atom probe tomography, *Acta Mater.*, **6**: 4696–4706 (2013); https://doi.org/10.1016/j.actamat.2013.04.059

16. K.M. Youssef, A.J. Zaddach, C. Niu, D.L. Irving, and C.C. Koch, A novel low-density, high-hardness, high-entropy alloy with close-packed single-phase nanocrystalline structures, *Mater. Res. Lett.*, **3**, No. 2: 95–99 (2015); https://doi.org/10.1080/21663831.2014.985855

17. N. Nayan, G. Singh, S.V.S.N. Murty, A.K. Jha, B. Pant, K.M. George, and U. Ramamurty, Hot deformation behaviour and microstructure control in AlCrCuNiFeCo

high entropy alloy, *Intermetallics*, **55**: 145–153 (2014);
https://doi.org/10.1016/j.intermet.2014.07.019

18. C.S. Babu, N.T.B.N. Koundinya, K. Sivaprasad, and J.A. Szpunar, Thermal analysis and nanoindentaion studies on nanocrystalline AlCrNiFeZn high entropy alloy, *Procedia Materials Science*, **6**: 641–647 (2014); https://doi.org/10.1016/j.mspro.2014.07.079

19. I. Volokitina, *J. Chemical Technology and Metallurgy*, **57**, No. 3: 631–636 (2022).

20. I.E. Volokitina and A.V. Volokitin, Changes in microstructure and mechanical properties of steel-copper wire during deformation, *Metallurgist*, **67**: 232–239 (2023); https://doi.org/10.1007/s11015-023-01510-7

21. A.V. Volokitin, I.E. Volokitina, and E.A. Panin, Thermomechanical treatment of stainless steel piston rings, *Prog. Phys. Met.*, **23**, No. 3: 411–437 (2022); https://doi.org/10.15407/ufm.23.03.411

22. A. Nurumgaliyev, T. Zhuniskaliyev, V. Shevko, Y. Mukhambetgaliyev, B. Kelamanov, Y. Kuatbay, A. Badikova, G. Yerekeyeva, and I. Volokitina, *Scientific Reports*, **14**, No. 1: 7456 (2024); https://doi.org/10.1038/s41598-024-57529-6

23. G. Kurapov, E. Orlova, I. Volokitina, and A. Turdaliev, *J. Chem. Technol. Metallurgy.*, **51**, No. 4: 451–457 (2016).

24. S. Lezhnev, I. Volokitina, and T. Koinov, *J. Chem. Technol. Metallurgy.*, **49**, No. 6: 621 (2014).

25. I.E. Volokitina, A.V. Volokitin E. Panin, T. Fedorova, D. Lawrinuk, A. Kolesnikov, A. Yerzhanov, Z. Gelmanova, and Y. Liseitsev, *Case Studies in Construction Materials*, **19**: e02609 (2023); https://doi.org/10.1016/j.cscm.2023.e02609

26. S.V. Starenchenko, Eh.V. Kozlov, and V.A. Starenchenko, *Zakonomernosti Termicheskogo Fazovogo Perekhoda Poryadok−Besporyadok v Splavakh so Sverkhstrukturami $L1_2$, $L1_2(M)$, $L1_2(MM)$, $D1_a$* (Tomsk: NTL: 2007) (in Russian).

27. A.A. Smirnov, Uporyadochenie Splavov pri Vysokikh Davleniyakh. *Metally, Elektrony, Reshyotka* (Kiev: Naukova Dumka: 1975), pp. 28–47 (in Russian).

28. F.Ch. Niks and V. Shokli, Prevrashcheniya v splavakh, *Uspekhi Fizicheskikh Nauk*, **20**, No. 3: 344–409 (1938) (in Russian); https://doi.org/10.3367/UFNr.0020.193807c.0344

29. F.Ch. Niks and V. Shokli, Prevrashcheniya v splavakh, *Uspekhi Fizicheskikh Nauk*, **20**, No. 4: 536–586 (1938) (in Russian); https://doi.org/10.3367/UFNr.0020.193808c.0536

30. M.A. Krivoglaz and A.A. Smirnov, *Teoriya Uporyadochivayushchikhsya Splavov* (Moskva: Fizmatgiz: 1958) (in Russian).

31. T. Muto and Yu. Takagi, The theory of order−disorder transitions in alloys, *Solid State Physics*, **1**: 193–282 (1955); https://doi.org/10.1016/S0081-1947(08)60679-7

32. A.A. Smirnov, *Molekulyarno-Kineticheskaya Teoriya Metallov* (Moskva: Nauka: 1966) (in Russian).

33. A.A. Smirnov, *Obobshchennaya Teoriya Uporyadocheniya Splavov* (Kiev: Naukova Dumka: 1986) (in Russian).

34. A.A. Smirnov, *Teoriya Vakansiy v Metallakh i Splavakh i Yeyo Primenenie k Splavam Vychitaniya* (Kiev: Naukova Dumka: 1993) (in Russian).

35. N.S. Stoloff and R.G. Davies, The mechanical properties of ordered alloys, *Prog. Mater. Sci.*, **13**: 1–84 (1968); https://doi.org/10.1016/0079-6425(68)90018-2

36. N.S. Stoloff, Ordered alloys — physical metallurgy and structural applications, *Int. Metals Reviews*, **29**, No. 1: 123–135 (1984); https://doi.org/10.1179/imtr.1984.29.1.123

37. V.I. Iveronova and A.A. Katsnel'son, *Blizhniy Poryadok v Tverdykh Rastvorakh* (Moskva: Nauka: 1977) (in Russian).

38. A.G. Khachaturyan, Ordering in substitutional and interstitial solid solutions, *Prog. Mater. Sci.*, **22**, Nos. 1–2: 1–150 (1978); https://doi.org/10.1016/0079-6425(78)90003-8

39. A.G. Khachaturyan, *Theory of Structural Transformations in Solids* (Mineola, NY: Dover Publications, Inc.: 2008).

40. D.A. Porter, K.E. Easterling, and M.Y. Sherif, *Phase Transformations in Metals and Alloys* (Boca Raton–London–New York: Taylor & Francis–CRC Press: 2009).

41. N.M. Matveeva and Eh.V. Kozlov, *Uporyadochennyye Fazy v Metallicheskikh Sistemakh* (Moskva: Nauka: 1989) (in Russian).

42. Eh.V. Kozlov, V.M. Dementyev, N.M. Kormin, and D.M. Shtern, *Struktury i Stabil'nost' Uporyadochennykh Faz* (Tomsk: Izd-vo Tomskogo Universiteta: 1994) (in Russian).

43. F. Reynaud, Order–disorder transitions in substitutional solid solutions, *physica status solidi A*, **72**: 11–60 (1982); https://doi.org/10.1002/pssa.2210720102

44. L.E. Tanner and H.J. Leamy, The microstructure of order–disorder transitions, *Order–Disorder Transformation in Alloys* (Ed. H. Warlimont) (Berlin: 1974), pp. 180–239; https://doi.org/10.1007/978-3-642-80840-1_8

45. A.I. Potekaev, I.I. Naumov, V.V. Kulagina, V.N. Udodov, O.I. Velikokhatnyy, and S.V. Eremeev, *Estestvennyye Dlinnoperiodicheskie Nanostruktury* (Tomsk: NTL: 2002) (in Russian).

46. L. Guttman, Order–disorder phenomenon in metals, *Solid State Physics* (Eds. F. Seitz and D. Turnbull) (New York: Academic Press Inc.: 1956), p. 145; https://doi.org/10.1016/S0081-1947(08)60133-2

47. S. Ogawa, M. Hirabayashi, D. Watanabe, and H. Iwasaki, *Long-Period Ordered Alloys* (Tokyo: Agne Gijutsu Center Inc.: 1997).

48. V.G. Vaks, Kinetics of phase separation and ordering in alloys, *Physics Reports*, **391**, Nos. 3–6: 157–242 (2004); https://doi.org/10.1016/j.physrep.2003.10.005

49. V.N. Bugaev and V.A. Tatarenko, *Interaction and Arrangement of Atoms in Interstitial Solid Solutions Based on Close-Packed Metals* (Kiev: Naukova Dumka: 1989) (in Russian).

50. V.A. Tatarenko and T.M. Radchenko, Direct and indirect methods of the analysis of interatomic interaction and kinetics of a relaxation of the short-range order in close-packed substitutional (interstitial) solid solutions, *Usp. Fiz. Met.*, **3**, No. 2: 111–236 (2002) (in Ukrainian); https://doi.org/10.15407/ufm.03.02.111

51. T.M. Radchenko and V.A. Tatarenko, Fe–Ni alloys at high pressures and temperatures: statistical thermodynamics and kinetics of the $L1_2$ or $D0_{19}$ atomic order, *Usp. Fiz. Met.*, **9**, No. 1: 1–170 (2008) (in Ukrainian); https://doi.org/10.15407/ufm.09.01.001

52. V.A. Tatarenko, T.M. Radchenko, A.Yu. Naumuk, and B.M. Mordyuk, Statistical-thermodynamic models of the Ni–Al-based ordering phases ($L1_2$, $L1_0$, $B2$): role of magnetic Ni-atoms' contribution, *Prog. Phys. Met.*, **25**, No. 1: 3–26 (2024); https://doi.org/10.15407/ufm.25.01.003

53. V.A. Tatarenko, T.M. Radchenko, A.Yu. Naumuk, and B.M. Mordyuk, Parameterization of the diffusion characteristics of atomic-order relaxation kinetics in Ni–Al alloys, *Prog. Phys. Met.*, **26**, No. 1: 3–25 (2025); https://doi.org/10.15407/ufm.26.01.003

54. An.D. Zolotarenko, Ol.D. Zolotarenko, Z.A. Matysina, N.A. Shvachko, N.Y. Akhanova, M. Ualkhanova, D.V. Schur, M.T. Gabdullin, M.T. Kartel, Yu.M. Solonin, Yu.I. Zhirko, D.V. Ismailov, A.D. Zolotarenko, and I.V. Zagorulko, Hydrogen in compounds

and alloys with *A*15 Structure, *Prog. Phys. Met.*, **24**, No. 4: 654–685 (2023); https://doi.org/10.15407/ufm.24.04.654

55. An.D. Zolotarenko, Ol.D. Zolotarenko, Z.A. Matysina, N.A. Shvachko, N.Y. Akhanova, M. Ualkhanova, D.V. Schur, M.T. Gabdullin, Yu.I. Zhirko, Yu.M. Solonin, V.V. Lobanov, D.V. Ismailov, A.D. Zolotarenko, and I.V. Zagorulko, On the solubility of hydrogen in metals and alloy, *Prog. Phys. Met.*, **24**, No. 3: 415–445 (2023); https://doi.org/10.15407/ufm.24.03.415

56. G.C. Kuczynski, R.E. Hochman, and M. Doyama, Study of the kinetics of ordering in the alloy AuCu, *J. Appl. Phys.*, **26**: 871–878 (1955); https://doi.org/10.1063/1.1722112

57. A. Kussman and K. Jessen, Magnetische und dilatometrische messungen zur umwandlungskinetik der eisen–palladium legierungen, *Zeitschrift für Metallkunde*, **54**: 504–510 (1963); https://doi.org/10.1515/ijmr-1963-540902

58. E. Raub and G. Worwag, Über Gold–Palladium–Kupfer Legierungen, *Zeitschrift für Metallkunde*, **46**: 119–128 (1955); https://doi.org/10.1515/ijmr-1955-460208

59. H. Mughrabi, T. Ungar, W. Kienle, and M. Wilkens, Long-range internal stresses and asymmetric X-ray line-broadening in tensile-deformed [001]-orientated copper single crystals, *Phil. Mag. A*, **53**: 793–815 (1986); https://doi.org/10.1080/01418618608245293

60. B.A. Greenberg, O.V. Antonova, L.E. Karkina, A.B. Notkin, and M.V. Ponomarev, Dislocation transformation and the anomalies of deformation characteristics in TiAl—IV. Observation of blocked dislocations, *Acta Met. Matter.*, **40**: 815–830 (1992); https://doi.org/10.1016/0956-7151(92)90024-9

61. C. Creatu and E. Lingen, Coloured gold alloys, *Gold Bulletin*, **32**: 115–126 (1999); https://doi.org/10.1007/BF03214796

62. K. Ohshima and D. Watanabe, Electron diffraction study of short-range-order diffuse scattering from disordered Cu–Pd and Cu–Pt alloys, *Acta Cryst. A*, **29**: 520–526 (1973); https://doi.org/10.1107/S0567739473001300

63. A. Naizabekov, A. Arbuz, S. Lezhnev, E. Panin, and I. Volokitina, The development and testing of a new method of qualitative analysis of the microstructure quality, for example of steel AISI 321 subjected to radial shear rolling, *Physica Scripta*, **94**, No. 10: 105702 (2019); https://doi.org/10.1088/1402-4896/ab1e6e

64. I.E. Volokitina and G.G. Kurapov, *Metal Sci. Heat Treat.*, **59**, Nos. 11–12: 786 (2018); https://doi.org/10.1007/s11041-018-0227-0

65. A.V. Volokitin, M.A. Latypova, A.T. Turdaliev, and O.G. Kolesnikova, Progress in additive manufacturing, *Prog. Phys. Met.*, **24**, No. 4: 686–714 (2023); https://doi.org/10.15407/ufm.24.04.686

66. A.T. Turdaliev, M.A. Latypova, and E.N. Reshotkina, Synthetic-hydroxyapatite-based coatings on the ultrafine-grained titanium and zirconium surface, *Prog. Phys. Met.*, **24**, No. 4: 792–818 (2023); https://doi.org/10.15407/ufm.24.04.792

67. I.E. Volokitina and A.V. Volokitin, *Phys. Metals Metallogr.*, **119**, No. 9: 917–921 (2018); https://doi.org/10.1134/S0031918X18090132

68. I.E. Volokitina, A.V. Volokitin, M.A. Latypova, V.V. Chigirinsky, and A.S. Kolesnikov, Effect of controlled rolling on the structural and phase transformations, *Prog. Phys. Met.*, **24**, No. 1: 132–156 (2023); https://doi.org/10.15407/ufm.24.01.132

69. I. Volokitina, B. Sapargaliyeva, A. Agabekova, A. Volokitin, S. Syrlybekkyzy, A. Kolesnikov, G. Ulyeva, A. Yerzhanov, and P. Kozlov, Study of changes in microstruc-

ture and metal interface Cu/Al during bimetallic construction wire straining, *Case Studies Construct. Mater.*, **18**: e02162 (2023); https://doi.org/10.1016/j.cscm.2023.e02162

70. A. Volokitin, I. Volokitina, and E. Panin, Martensitic transformation in aisi-316 austenitic steel during thermomechanical processing, *Metallography, Microstructure, and Analysis*, **11**, No. 4: 673–675 (2022); https://doi.org/10.1007/s13632-022-00877-4

71. A. Volokitin, A. Naizabekov, I. Volokitina, and A. Kolesnikov, *J. Chemical Technoogy and Metallurgy*, **57**: 809 (2022).

72. A.B. Naizabekov, S.N. Lezhnev, and I. Volokitina, Change in copper microstructure and mechanical properties with deformation in an equal channel stepped die, *Metal Sci. Heat Treat.*, **57**, Nos. 5–6: 254–260 (2015); https://doi.org/10.1007/s11041-015-9870-x

73. I. Volokitina, B. Sapargaliyeva, A. Agabekova, S. Syrlybekkyzy, A. Volokitin, L. Nurshakhanova, F. Nurbaeva, A. Kolesnikov, G. Sabyrbayeva, A. Izbassar, O. Kolesnikova, Y. Liseitsev, and S. Vavrenyuk, *Case Studies Construct. Mater.*, **19**: e02256 (2023); https://doi.org/10.1016/j.cscm.2023.e02256

74. S.N. Lezhnev, I. Volokitina, and A.V. Volokitin, Evolution of microstructure and mechanical properties of steel in the course of pressing–drawing, *Phys. Metals Metallogr.*, **118**, No. 11: 1167–1170 (2017); https://doi.org/10.1134/S0031918X17110072

75. S. Lezhnev, E. Panin, and I. Volokitina, Research of combined process "rolling-pressing" influence on the microstructure and mechanical properties of aluminium, *Adv. Mater. Res.*, **814**: 68–75 (2013); https://doi.org/10.4028/www.scientific.net/AMR.814.68

76. S. Bärthlein, E. Winning, G.L. Hart, and S. Müller, Stability and instability of long-period superstructures in binary Cu–Pd alloys: a first principles study, *Acta Mater.*, **57**: 1660–1665 (2009); https://doi.org/10.1016/j.actamat.2008.12.013

77. H. Okamoto, D. Chakrabarti, D. Laughlin, and T. Massalski, The Au–Cu (gold–copper) system, *J. Phase Equilibria*, **8**: 454–474 (1987); https://doi.org/10.1007/BF02893155

78. A. Verma, J. Singh, M. Sundararaman, and N. Wanderka, Resistivity and transmission electron microscopy investigations of ordering transformation in stoichiometric $Ni_2(Cr_{0.5}Mo_{0.5})$ alloy, *Metallurgical and Materials Transactions A*, **43**: 3078–3085 (2012); https://doi.org/10.1007/s11661-012-1145-1

79. D. Broddin, G.V. Tendeloo, J.V. Landuyt, and S. Amelinckx, Two-dimensional long period structures in Cu–Pd. A study of the mechanism of the transition from a one-dimensional LPS to a two-dimensional LPS, *Philosophical Magazine A*, **59**: 47–61 (1989); https://doi.org/10.1080/01418618908220330

80. M.E. Fisher and W. Selke, Infinitely many commensurate phases in a simple ising model, *Phys. Rev. Lett.*, **44**: 1502–1505 (1980); https://doi.org/10.1103/PhysRevLett.44.1502

81. S. Ogawa and D. Watanabe, Electron diffraction study on the ordered alloy CuAu, *J. Phys. Soc. Jpn.*, **9**: 475–488 (1954); https://doi.org/10.1143/JPSJ.9.475

82. S. Yamaguchi, D. Watanabe, and S. Ogawa, *J. Phys. Soc. Jpn.*, **17**: 1030–1041 (1962); https://doi.org/10.1143/JPSJ.17.1030

83. H. Sato and R.S. Toth, Long-period superlattices in alloys. II, *Phys. Rev.*, **127**: 469–484 (1962); https://doi.org/10.1103/PhysRev.127.469

84. O. Terasaki, Direct observation of 'domain like' atomic arrangement of incommensurate 2d $Au_{3+}Zn$ by high-voltage-high-resolution electron microscopy, *J. Physics C: Solid State Physics*, **14**: L933 (1981); https://doi.org/10.1088/0022-3719/14/31/002

85. D. Watanabe, M. Hirabayashi, and S. Ogawa, On the super-structure of the alloy Cu_3Pd, *Acta Crystallogr.*, **8**: 510−512 (1955); https://doi.org/10.1107/S0365110X55001576

86. M. Hirabayashi and S. Ogawa, On the superstructure of the ordered alloy Cu_3Pd II. X-ray diffraction study, *J. Phys. Soc. Jpn.*, **12**: 259−271 (1957); https://doi.org/10.1143/JPSJ.12.259

87. H. Sato and R.S. Toth, Effect of additional elements on the period of CuAu II and the origin of the long-period superlattice, *Phys. Rev.*, **124**: 1833−1847 (1961) https://doi.org/10.1103/PhysRev.124.1833

88. C.H. Johansson and J.O. Linde, Gitterstruktur und elektrisches Leitvermц-gen der Mischkristallreihen Au−Cu, Pd−Cu und Pt−Cu, *Annalen der Physik*, **387**: 449−478 (1927); https://doi.org/10.1002/andp.19273870402

89. F.C. Nix and W. Shockley, *Rev. Mod. Phys.*, **10**: 1−71 (1938).

90. F.W. Jones and C. Sykes, The superlattice in β brass, Proceedings of the Royal Society of London A: Mathematical, *Physical and Engineering Sciences*, **161**: 440−446 (1937); https://doi.org/10.1098/rspa.1937.0154

91. S. Ogawa and D. Watanabe, On the structure of CuAu II revealed by electron diffraction, *Acta Crystallogr.*, **7**: 377−378 (1954); https://doi.org/10.1107/S0365110X54001077

92. J.B. Newkirk, Order−disorder transformation in Cu−Au alloys near the composition CuAu, *JOM*, **5**: 823−826 (1953); https://doi.org/10.1007/BF03397552

93. D. Watanabe, On the superstructure of the ordered alloy Cu_3Pd. III. High temperature electron diffraction study, *J. Phys. Soc. Jpn.*, **14**: 436−443 (1959); https://doi.org/10.1143/JPSJ.14.436

94. J.F. Jaumot and A. Sawatzky, *Acta Metall.*, **4**: 118−126 (1956); https://doi.org/10.1016/0001-6160(56)90130-4

95. F.E. Jaumot and A. Sawatzky, An isothermal anneal study of quenched and cold-worked copper-palladium alloys, *Acta Metall.*, **4**: 118−126 (1956); https://doi.org/10.1016/0001-6160(56)90131-6

96. K. Fujiwara, M. Hirabayashi, D. Watanabe, and S. Ogawa, Study on the ordered alloy Ag_3Mg, *J. Phys. Soc. Jpn.*, **13**: 167−174 (1958); https://doi.org/10.1143/JPSJ.13.167

97. K. Fujiwara, On the period of out-of-step of ordered alloys with anti-phase domain structure, *J. Phys. Soc. Jpn.*, **12**: 7−13 (1957); https://doi.org/10.1143/JPSJ.12.7

98. J.A. Rayne, Heat capacity of Cu_3Au below 4.2 K, *Phys. Rev.*, **108**: 649−651 (1957); https://doi.org/10.1103/PhysRev.108.649

99. P. Pério and M. Tournarie, Diffraction par les antiphase périodiques a une et deux directions du type $AuCu_3$, *Acta Crystallogr.*, **12**: 1032−1038 (1959); https://doi.org/10.1107/S0365110X59002882

100. J.M. Cowley, Short- and long-range order parameters in disordered solid solutions, *Phys. Rev.*, **120**: 1648−1657 (1960); https://doi.org/10.1103/PhysRev.120.1648

101. K. Okamura, Lattice Modulation in the long period ordered alloys studied by X-ray diffraction. III. $Cu_3Pd(\alpha'')$, *J. Phys. Soc. Jpn.*, **28**: 1005−1014 (1970);

https://doi.org/10.1143/JPSJ.28.1005

102. A. Gangulee and S.C. Moss, Long range order in Ag$_3$Mg, *J. Applied Crystal-lography*, **1**: 61–67 (1968);
https://doi.org/10.1107/S0021889868005017

103. R. Kubiak and M. Wolcyrz, Twinning observed by x-ray diffraction in AuCu-ordered alloys, *J. Less Common Metals*, **160**: 101–107 (1990);
https://doi.org/10.1016/0022-5088(90)90111-V

104. C. Gammer, C. Mangler, C. Rentenberger, and H. Karnthaler, Quantitative local profile analysis of nanomaterials by electron diffraction, *Scripta Mater.*, **63**: 312–315 (2010);
https://doi.org/10.1016/j.scriptamat.2010.04.019

105. M. Marcinkowski and L. Zwell, Transmission electron microscopy study of the off-stoichiometric Cu$_3$Au superlattices, *Acta Metall.*, **11**: 373–390 (1963);
https://doi.org/10.1016/0001-6160(63)90162-7

106. H. Sato and R.S. Toth, Effect of additional elements on the period of CuAu*II* and the origin of the long-period superlattice, *Phys. Rev.*, **124**: 1833–1847 (1961);
https://doi.org/10.1103/physrev.124.1833

107. G. Vanderschaeve, Étude en microscopie électronique d'un alliage possédant une surstructure a longue période: Ag$_3$Mg, *physica status solidi*, **36**: 103–117 (1969);
https://doi.org/10.1002/PSSB.19690360110

108. K. Hanhi, J. Mäki, and P. Paalassalo, Electron microscopic investigation of long period order in Ag$_3$Mg, *Acta Metall.*, **19**: 15–20 (1971);
https://doi.org/10.1016/0001-6160(71)90156-8

109. J. Kakinoki and T. Minagawa, The one-dimensional anti-phase domain struc-tures. II. Refinement of Fujiwara's method of the analysis of the structure with a non-integral value for the half period, M, *Acta Crystallogr.*, **28**: 120–133 (1972);
https://doi.org/10.1107/S0567739472000282

110. G. van Tendeloo and S. Amelinckx, *Acta Crystallogr.*, **30**: 431–440 (1974);
https://doi.org/10.1107/S0567739474000933

111. K. Mihama, Growth and structure of AuCu II particles, *J. Phys. Soc. Jpn.*, **31**: 1677–1682 (1971);
https://doi.org/10.1143/JPSJ.31.1677

112. L. Howe, M. Rainville, and E. Schulson, Transmission electron microscopy inves-tigations of ordered Zr$_3$Al, *J. Nuclear Materials*, **50**: 139–154 (1974);
https://doi.org/10.1016/0022-3115(74)90151-2

113. R. De Ridder, G. van Tendeloo, and S. Amelinckx, A cluster model for the transition from the short-range order to the long-range order state in f.c.c. based binary systems and its study by means of electron diffraction, *Acta Crystallogr.*, **32**: 216–224 (1976);
https://doi.org/10.1107/S0567739476000508

114. C. Leroux, A. Loiseau, M.C. Cadeville, D. Broddin, and G.V. Tendeloo, Order–dis-order transformation in Co$_{30}$Pt$_{70}$ alloy: evidence of wetting from the anti-phase boundaries, *J. Physics: Condensed Matter*, **2**: 3479 (1990);
https://doi.org/10.1088/0953-8984/2/15/005

115. S. Takeda, J. Kulik, and D. de Fontaine, One-dimensional long-period super-structures in Cu$_3$Pd observed by high-resolution electron microscopy, *J. Physics F*, **18**: 1387 (1988);
https://doi.org/10.1088/0305-4608/18/7/009

116. D. Geist, C. Gammer, C. Mangler, C. Rentenberger, and H. Karnthaler, Electron microscopy of severely deformed $L1_2$ intermetallics, *Philosophical Magazine*, **90**: 4635–4645 (2010);

https://doi.org/10.1080/14786435.2010.482178

117. I. Volokitina, N. Vasilyeva, R. Fediuk, and A. Kolesnikov, Hardening of bimetallic wires from secondary materials used in the construction of power lines, *Materials*, **15**, No. 11: 3975 (2022);
https://doi.org/10.3390/ma15113975

118. I.E. Volokitina, A.I. Denissova, A.V. Volokitin, and E.A. Panin, Methods for obtaining a gradient structure, *Prog. Phys. Met.*, **25**, No. 1: 132–160 (2024);
https://doi.org/10.15407/ufm.25.01.132

119. I. Volokitina, A. Volokitin, A. Denissova, T. Fedorova, D. Lawrinuk, A. Kolesnikov, A. Yerzhanov, Y. Kuatbay, and Y. Liseitsev, Effect of thermomechanical processing of building stainless wire to increase its durability, *Case Studies Construct. Mater.*, **19**: e02346 (2023);
https://doi.org/10.1016/j.cscm.2023.e02346

120. I. Volokitina, A. Volokitin, and D. Kuis, *J. Chemical Technology and Metallurgy*, **56**: 643 (2021).

121. I.E. Volokitina, Effect of cryogenic cooling after ecap on mechanical properties of aluminum alloy D16, *Metal Sci. Heat Treat.*, **61**: 234 (2019);
https://doi.org/10.1007/s11041-019-00406-1

122. A.B. Nayzabekov and I.E. Volokitina, Effect of the initial structural state of Cr−Mo high-temperature steel on mechanical properties after equal-channel angular pressinga, *Phys. Metals Metallogr.*, **120**, No. 2: 177–183 (2019);
https://doi.org/10.1134/S0031918X19020133

123. S. Lezhnev and A. Naizabekov, New combined process "pressing-drawing" and impact on properties of deformable aluminum wire, *Procedia Engineering*, **81**: 1505–1510 (2014);
https://doi.org/10.1016/j.proeng.2014.10.181

124. S. Lezhnev, A. Naizabekov, and E. Panin, Influence of combined process "rolling-pressing" on microstructure and mechanical properties of copper, *Procedia Engineering*, **81**: 1499–1504 (2014);
https://doi.org/10.1016/j.proeng.2014.10.180

125. I.E. Volokitina, Effect of preliminary heat treatment on deformation of brass by the method of ECAP, *Metal Sci. Heat Treat.*, **63**, Nos. 3–4: 163–167 (2021);
https://doi.org/10.1007/s11041-021-00664-y

126. D.A. Sinitsin, A.E.M.M. Elrefaei, A.O. Glazachev, D.V. Kuznetsov, A.A. Parfenova, I.E. Volokitina, E.I. Kayumova, and I.V. Nedoseko, *Construction Materials and Products*, **6**, No. 6: 2 (2023);
https://doi.org/10.58224/2618-7183-2023-6-6-2

127. Z.S. Gelmanova, B.A. Bazarov, A.V. Mezentseva, A.N. Konakbaeva, and A.K. Toleshov, *Mining Informational and Analytical Bulletin*, **2**: 184–198 (2021);
https://doi.org/10.25018/0236-1493-2021-21-0-184-198

128. V.V. Chigirinsky, Yu.S. Kresanov, and I.Y. Volokitina, Study of kinematic and deformation parameters of rolling of compressor blade workpieces, *Metallofiz. Noveishie Tekhnol.*, **45**, No. 5: 631–646 (2023);
https://doi.org/10.15407/mfint.45.05.0631

129. I. Volokitina, A. Volokitin, E. Panin, and B. Makhmutov, Symmetrical martensite distribution in wire using cryogenic cooling, *Symmetry*, **16**, No. 9: 1174 (2024);
https://doi.org/10.3390/sym16091174

130. V.V. Chigirinsky, Y.S. Kresanov, and I.E. Volokitina, Experimental study of energypower parameters of billet rolling of compressor blades of aircraft engines, Metallofiz. *Noveishie Tekhnol.*, **45**, No. 4: 467–479 (2023);
https://doi.org/10.15407/mfint.45.04.0467

131. M.-R. Chen, S.-J. Lin, J.-W. Yeh, S.-K. Chen, Y.-S. Huang, and C.-P. Tu, Micro-structure and properties of $Al_{0.5}CoCrCuFeNiTi_x$ ($x = 0$−2.0) high-entropy alloys, *Materials Transactions*, **47**: 1395−1401 (2006); https://doi.org/10.2320/matertrans.47.1395

132. M.-R. Chen, S.-J. Lin, J.-W. Yeh, M.-H. Chuang, S.-K. Chen, and Y.-S. Huang, Effect of vanadium addition on the microstructure, hardness, and wear resistance of $Al_{0.5}CoCrCuFeNi$ high-entropy alloy, *Metallurgical and Materials Transactions A*, **37**: 1363−1369 (2006); https://doi.org/10.1007/s11661-006-0081-3

133. A. Chbihi, X. Sauvage, C. Genevois, D. Blavette, D. Gunderov, and A. Popov, Optimization of the magnetic properties of FePd alloys by severe plastic deforma-tion, *Advanced Engineering Materials*, **12**: 708−713 (2010); https://doi.org/10.1002/adem.200900326

134. A. Naizabekov, I. Volokitina, A. Volokitin, and E. Panin, Structure and mechanical properties of steel in the process "pressing−drawing", *J. Materials Engineering and Performance*, **28**, No. 3: 1762 (2019); https://doi.org/10.1007/s11665-019-3880-6

135. I. Volokitina, A. Volokitin, and E. Panin, Gradient microstructure formation in carbon steel bars, *J. Materials Research and Technology*, **31**: 2985−2993 (2024); https://doi.org/10.1016/j.jmrt.2024.07.038

136. I.E. Volokitina, Evolution of the microstructure and mechanical properties of cop-per under ECAP with intense cooling, *Metal Sci. Heat Treat.*, **62**: 253−258 (2020); https://doi.org/10.1007/s11041-020-00544-x

137. I. Volokitina, A. Volokitin, and B. Makhmutov, Formation of symmetric gradient microstructure in carbon steel bars, *Symmetry*, **16**, No. 8: 997 (2024); https://doi.org/10.3390/sym16080997

138. X.Z. Liao, Y.H. Zhao, Y.T. Zhu, R.Z. Valiev, and D.V. Gunderov, Grainsize effect on the deformation mechanisms of nanostructured copper processed by high-pres-sure torsion, *J. Applied Physics*, **96**: 636−640 (2004); https://doi.org/10.1063/1.1757035

139. A.V. Volokitin, I. Volokitina, T.D. Fedorova, M.A. Latypova, and D.N. Lavrinyuk, Analysis of the twisting effect in an equal-channel stepped die and drawing on copper wire mechanical properties, *Metallurgist*, **68**, No. 4: 530−536 (2024); https://doi.org/10.1007/s11015-024-01756-9

140. I.E. Volokitina and A.V. Volokitin, Effect of annealing temperature on microstruc-ture and properties of stainless steel rings after high-pressure torsion, *Metal-lurgist*, **68**, No. 1: 52−58 (2024); https://doi.org/10.1007/s11015-024-01703-8

141. E.F. Talantsev, *d*-Wave superconducting gap symmetry as a model for $Nb_{1-x}Mo_xB_2$ ($x = 0.25$; 1.0) and WB_2 diborides, *Symmetry*, **15**, No. 4: 812 (2023); https://doi.org/10.3390/sym15040812

142. M.M. Nofal, R. Sai, R.S. Shawish, and M.A. Alaqeel, An insight of the theoretical physics of Ru-alloyed iron pyrite studied for energy generation, *Symmetry*, **14**, No. 11: 2252 (2022); https://doi.org/10.3390/sym14112252

143. F. Yu and Y. Liu, *Symmetry*, **11**, No. 8: 972 (2019); https://doi.org/10.3390/sym11080972

144. J.E. Taylor, E.G. Teich, P.F. Damasceno, Y. Kallus, and M. Senechal, DFT calcu-lations of the structural, mechanical, and electronic properties of TiV alloy under high pressure, *Symmetry*, **9**, No. 9: 188 (2017); https://doi.org/10.3390/sym9090188

145. B. Jang, S. Riemer, and G.M. Pastor, Chiral magnetic interactions in small Fe clus-

ters triggered by symmetry-breaking adatoms, *Symmetry*, **15**, No. 2: 397 (2023); https://doi.org/10.3390/sym15020397

146. R. Valiev, A. Korznikov, and R. Mulyukov, Structure and properties of ultrafine-grained materials produced by severe plastic deformation, *Mater. Sci. Eng. A*, **168**: 141–148 (1993); https://doi.org/10.1016/0921-5093(93)90717-S

147. A. Zhilyaev, S. Lee, G. Nurislamova, R. Valiev, and T. Langdon, Microhardness and microstructural evolution in pure nickel during high-pressure torsion, *Scripta Mater.*, **44**: 2753–2758 (2001); https://doi.org/10.1016/S1359-6462(01)00955-1

148. X. Zhang, Y. Li, M. Kaufman, and M. Loretto, The structure and origin of boundaries between antiphase regions in $L1_0$ intermetallics, *Acta Mater.*, **44**: 3735–3747 (1996); https://doi.org/10.1016/1359-6454(95)00454-8

149. H. Rösner, N. Boucharat, J. Markmann, K. Padmanabhan, and G. Wilde, *Mater. Sci. Eng. A*, **525**: 102–106 (2009); https://doi.org/10.1016/j.msea.2009.06.035

150. T.M. Radchenko and V.A. Tatarenko, Statistical thermodynamics and kinetics of atomic order in doped graphene. I. Substitutional solution, *Nanosistemi, Nanomateriali, Nanotehnologii*, **6**, No. 3: 867–910 (2008) (in Ukrainian).

151. T.M. Radchenko and V.A. Tatarenko, Statistical thermodynamics and kinetics of atomic order in doped graphene. II. Interstitial solution, *Nanosistemi, Nanomateriali, Nanotehnologii*, **8**, No. 3: 619–650 (2010) (in Ukrainian).

152. T.M. Radchenko, Substitutional superstructures in the doped graphene lattice, *Metallofiz. Noveishie Tekhnol.*, **30**, No. 8: 1021–1026 (2008) (in Ukrainian).

153. T.M. Radchenko and V.A. Tatarenko, Statistical thermodynamics and kinetics of long-range order in metal-doped graphene, *Solid State Phenomena*, **150**: 43–72 (2009); https://doi.org/10.4028/www.scientific.net/SSP.150.43

154. T.M. Radchenko and V.A. Tatarenko, Kinetics of atomic ordering in metal-doped graphene, *Solid State Sci.*, **12**, No. 2: 204–209 (2010); https://doi.org/10.1016/j.solidstatesciences.2009.05.027

155. T.M. Radchenko and V.A. Tatarenko, A statistical-thermodynamic analysis of stably ordered substitutional structures in graphene, *Physica E*, **42**, No. 8: 2047–2054 (2010); https://doi.org/10.1016/j.physe.2010.03.024

156. I.Yu. Sagalyanov, Yu.I. Prylutskyy, T.M. Radchenko, and V.A. Tatarenko, Graphene systems: methods of fabrication and treatment, structure formation, and functional properties, *Usp. Fiz. Met.*, **11**, No. 1: 95–138 (2010) (in Ukrainian); https://doi.org/10.15407/ufm.11.01.095

157. T.M. Radchenko and V.A. Tatarenko, Stable superstructures in a binary honeycomblattice gas, *Int. J. Hydrogen Energy*, **36**, No. 1: 1338–1343 (2011); https://doi.org/10.1016/j.ijhydene.2010.06.112

158. T.M. Radchenko and V.A. Tatarenko, Ordering kinetics of dopant atoms in graphene lattice with stoichiometric compositions of 1/3 and 1/6, *Materialwiss. Werkstofftech.*, **44**, Nos. 2–3: 231–238 (2013); https://doi.org/10.1002/mawe.201300094

159. T.M. Radchenko, V.A. Tatarenko, I.Yu. Sagalyanov, and Yu.I. Prylutskyy, Configurational effects in an electrical conductivity of a graphene layer with the distributed adsorbed atoms (K), *Nanosistemi, Nanomateriali, Nanotehnologii*, **13**, No. 2: 201–214 (2015).

160. T.M. Radchenko, I.Y. Sahalianov, V.A. Tatarenko, Y.I. Prylutskyy, P. Szroeder, M.

Kempiński, and W. Kempiński, The impact of uniaxial strain and defect pattern on magnetoelectronic and transport properties of graphene, *Handbook of Graphene*, *Vol. 1*: *Growth, Synthesis, and Functionalization* (Eds. E. Celasco, A.N. Chaika) (Beverly, MA: John Wiley & Sons, Inc., Scrivener Publishing LLC: 2019), Ch. 14, p. 451–502; https://doi.org/10.1002/9781119468455.ch14

161. T.M. Radchenko, V.A. Tatarenko, I.Yu. Sagalianov, and Yu.I. Prylutskyy, Configurations of structural defects in graphene and their effects on its transport properties, *Graphene: Mechanical Properties, Potential Applications and Electrochemical Performance* (Ed. Bruce T. Edwards) (New York: Nova Science Publishers, Inc.: 2014), Ch. 7, p. 219–259.

162. A.G. Solomenko, R.M. Balabai, T.M. Radchenko, and V.A. Tatarenko, Functionalization of quasi-two-dimensional materials: chemical and strain-induced modifications, *Prog. Phys. Met.*, **23**, No. 2: 147–238 (2022); https://doi.org/10.15407/ufm.23.02.147

163. S.P. Repetsky, I.G. Vyshyvana, S.P. Kruchinin, V.B. Molodkin, and V.V. Lizunov, Influence of the adsorbed atoms of potassium on an energy spectrum of graphene, *Metallofiz. Noveishie Tekhnol.*, **39**, No. 8: 1017–1022 (2017); https://doi.org/10.15407/mfint.39.08.1017

164. O.S. Skakunova, S.I. Olikhovskii, T.M. Radchenko, S.V. Lizunova, T.P. Vladimirova, and V.V. Lizunov, X-ray dynamical diffraction by quasi-monolayer graphene, *Scientific Reports*, **13**: 15950 (2023); https://doi.org/10.1038/s41598-023-43269-6

165. V.A. Tatarenko, O.V. Sobol', D.S. Leonov, Yu.A. Kunyts'kyy, and S.M. Bokoch, Statistical thermodynamics and physical kinetics of structural changes of quasi-binary solid solutions based on the close-packed simple lattices (according to the data about evolution of a pattern of scattering of waves of various kinds), *Usp. Fiz. Met.*, **12**, No. 1: 1–155 (2011) (in Ukrainian); https://doi.org/10.15407/ufm.12.01.001

166. V.A. Tatarenko and T.M. Radchenko, Kinetics of the hydrogen-isotopes short-range order in interstitial solid solutions h.c.p.-Ln–H(D,T), *Hydrogen Materials Science and Chemistry of Metal Hydrides: NATO Science Series, Series II: Mathematics, Physics and Chemistry* (Eds. T.N. Veziroglu, S.Yu. Zaginaichenko, D.V. Schur, and V.I. Trefilov) (Dordrecht, The Netherlands: Kluwer Academic Publishers: 2002), vol. 82, p. 123–132.

167. V.A. Tatarenko, T.M. Radchenko, and V.B. Molodkin, Microscopic characteristics of H diffusion and diffuse scattering of radiations in h.c.p.-*Ln*–H (from the data on electrical-resistivity relaxation), *Hydrogen Materials Science and Chemistry of Carbon Nanomaterials* (NATO Science Series, II: Mathe-matics, Physics and Chemistry) (Eds. T.N. Veziroglu, S.Yu. Zaginaichenko, D.V. Schur, B. Baranowski, A.P. Shpak, V.V. Skorokhod) (Dordrecht, The Netherlands: Kluwer Academic Publishers: 2004), vol. 172, p. 59–66; https://doi.org/10.1007/1-4020-2669-2_5

168. D.S. Leonov, T.M. Radchenko, V.A. Tatarenko, and Yu.A. Kunitsky, Kinetic parameters of migration of atoms and relaxation of scattering of different-type waves in the ordering fcc-Ni–Al alloy, *Metallofiz. Noveishie Tekhnol.*, **29**, No. 12: 1587–1602 (2007) (in Russian).

169. S.M. Bokoch, N.P. Kulish, T.M. Radchenko, S.P. Repetskiy, and V.A. Tatarenko, Parameters of a relaxation of an electrical resistance and diffuse scattering in binary substitutional solutions fcc-Ni–Mo, *Metallofiz. Noveishie Tekhnol.*, **24**, No. 5: 691–704 (2002) (in Russian).

170. S.M. Bokoch, M.P. Kulish, T.M. Radchenko, and V.A. Tatarenko, Kinetics of

short-range ordering of substitutional solid solutions (according to data on a scattering of various kinds of waves). I. Microscopic parameters of migration of atoms within f.c.c.-Ni−Mo in Fourier-representation, *Metallofiz. Noveishie Tekhnol.*, **26**, No. 3: 387−406 (2004) (in Russian).

171. S.M. Bokoch, M.P. Kulish, V.A. Tatarenko, and T.M. Radchenko, Kinetics of short-range ordering of substitutional solid solutions (according to data on a scattering of various kinds of waves). II. Parameters of atomic microdiffusion within f.c.c.-Ni−Mo, *Metallofiz. Noveishie Tekhnol.*, **26**, No. 4: 541−558 (2004) (in Russian).

172. D.S. Leonov, T.M. Radchenko, V.A. Tatarenko, and Yu.A. Kunitsky, Kinetics parameters of atomic migration and diffuse scattering of radiations within the f.c.c.-Ni−Al alloys, *Defect and Diffusion Forum*, **273−276**: 520−524 (2008); https://doi.org/10.4028/www.scientific.net/DDF.273-276.520

173. T.M. Radchenko and V.A. Tatarenko, Comments concerning parameters of the short-range order evolution determined from the data on kinetics of a heat-capacity relaxation for Lu−H alloy, *Hydrogen Materials Science and Chemistry of Carbon Nanomaterials. NATO Security through Science Series A: Chemistry and Biology* (Eds. T.N. Veziroglu, S.Yu. Zaginaichenko, D.V. Schur, B. Baranowski, A.P. Shpak, V.V. Skorokhod, A. Kale) (Dordrecht: Springer: 2007), p. 229−234; https://doi.org/10.1007/978-1-4020-5514-0_28

174. V.V. Lizunov, I.M. Melnyk, T.M. Radchenko, S.P. Repetsky, and V.A. Tatarenko, Influence of strong electron−electron correlations on the electrical conduction and magnetic properties of substitutional alloys as advanced functional spintronic materials, *Functional Magnetic and Spintronic Nanomaterials, NATO Science for Peace and Security Series B: Physics and Biophysics* (Eds. I. Vladymyrskyi, B. Hillebrands, A. Serha, D. Makarov, and O. Prokopenko) (Dordrecht: Springer: 2024), Ch. 1, p. 1−25; https://doi.org/10.1007/978-94-024-2254-2_1

175. K. Schubert, Crystal structures of beta brass like alloy phases, *Transactions of the Japan Institute of Metals*, **14**: 281−284 (1973); https://doi.org/10.2320/matertrans1960.14.281

176. H. Sato, R.S. Toth, and T.B. Massalski, *Alloying Behavior and Effects in Concentrated Solid Solutions* (New York: Gordon Breach Sci. Publ.: 1965).

177. J.C. Slater, Note on superlattices and brillouin zones, *Phys. Rev.*, **84**: 179−181 (1951); https://doi.org/10.1103/PhysRev.84.179

178. J.F. Nicholas, Effect of the Fermi energy on the stability of superlattices, *Proc. Physical Society. Section A*, **66**: 201 (1953); https://doi.org/10.1088/0370-1298/66/3/301

179. R.G. Jordan, X. Xu, S.L. Qiu, P.J. Durham, and G.Y. Guo, The long-period superlattice in CuAu II, *J. Physics: Condensed Matter*, **8**: 1503 (1996); https://doi.org/10.1088/0953-8984/8/10/020

180. Y. Sato, J.M. Sivertsen, and L.E. Toth, Low-temperature specific-heat study of Cu−Pd alloys, *Phys. Rev. B.*, **1**: 1402−1410 (1970); https://doi.org/10.1103/PhysRevB.1.1402

181. D. Watanabe, Study on the ordered alloys of gold−manganese system by electron diffraction. II. Au_4Mn, *J. Phys. Soc. Jpn.*, **15**: 1251−1257 (1960); https://doi.org/10.1143/JPSJ.15.1251

182. J.B. Cohen, A brief review of the properties of ordered alloys, *J. Materials Science*, **4**: 1012−1021 (1969); https://doi.org/10.1007/BF00555319

183. A. Zhilyaev, G. Nurislamova, B.-K. Kim, M. Baro, J. Szpunar, and T. Langdon, Experimental parameters influencing grain refinement and microstructural evolution during high-pressure torsion, *Acta Mater.*, **51**: 753−765 (2003); https://doi.org/10.1016/S1359-6454(02)00466-4

184. Y. Ivanisenko, W. Lojkowski, R. Valiev, and H.-J. Fecht, The mechanism of formation of nanostructure and dissolution of cementite in a pearlitic steel during; high pressure torsion, *Acta Mater.*, **51**: 5555−5570 (2003) https://doi.org/10.1016/S1359-6454(03)00419-1

185. G. Vanderschaeve, G. Coulon, and B. Escaig, Dislocation splitting in long period ordered Ag_3Mg and related deformation behaviour, *Physica Status Solidi*, **9**: 541−549 (1972); https://doi.org/10.1002/pssa.2210090217

186. K. Okamura, H. Iwasaki, and S. Ogawa, Lattice modulation in the long period ordered alloys studied by X-ray diffraction. II. CuAu II, *J. Phys. Soc. Jpn.*, **24**: 569−579 (1968); https://doi.org/10.1143/JPSJ.24.569

187. R.E. Scott, New complex phase in the copper−gold system, *J. Applied Physics*, **31**: 2112−2117 (1960); https://doi.org/10.1063/1.1735509

188. T. Sakai, A. Belyakov, R. Kaibyshev, H. Miura, and J. Jonas, Dynamic and post-dynamic recrystallization under hot, cold and severe plastic deformation conditions, *Prog. Mater. Sci.*, **60**: 130−207 (2014); https://doi.org/10.1016/j.pmatsci.2013.09.002

М.А. Латипова, З.С. Гельманова
Карагандинський індустріальний університет,
просп. Республіки, 30, 101400 Темиртау, Казахстан

УПОРЯДКОВНІ СПЛАВИ З МІКРО- ТА НАНОМАСШТАБНОЮ СТРУКТУРАМИ НА ОСНОВІ КУБІЧНИХ ҐРАТОК: МЕХАНІЧНІ ТА ТЕРМОДИНАМІЧНІ ВЛАСТИВОСТІ

У зв'язку з розвитком транспортної, хімічної, енергетичної індустрії, авіакосмічної техніки, суднобудування постає необхідність розроблення та створення нових матеріалів, здатних функціонувати в різноманітних умовах. До цих матеріалів належать атомарно впорядковані сплави на основі благородних металів, що мають особливі властивості, як-от висока корозійна стійкість, низький електроопір, відповідні магнітні й оптичні властивості. Водночас для їх практичного застосування дедалі більш затребуваним стає комплексне поєднання необхідних експлуатаційних характеристик, що забезпечують поряд з достатніми електрорезистивними й електроконтактними властивостями високі міцність і пластичність на додаток до корозійної стійкості. Також, безсумнівно, важливими залишаються простота хімічного складу створюваних або вдосконалюваних матеріалів, технологічність металургійного процесу і подальших виробничих переділів на наявному обладнанні.

Ключові слова: далекий атомний порядок, упорядковані сплави, кінетика, механізм деформації, мікроструктура.